Transcriptomic mapping of key reproductive and metabolic tissues and oocytes in mouse models of polycystic ovary syndrome

Qiaolin Deng (Qiaolin.Deng@ki.se)
Karolinska Institutet
Yu Pei
Sanjiv Risal
Hong Jiang
Jiang Lu
Eva Lindgren
Elisabet Stener-Victorin

Article

Keywords:

Posted Date: August 11th, 2022

DOI: https://doi.org/10.21203/rs.3.rs-1917590/v1

Transcriptomic mapping of key reproductive and metabolic tissues and oocytes in mouse models of polycystic ovary syndrome

Yu Pei[1,2,3], Sanjiv Risal[1,3], Hong Jiang[1], Haojiang Lu[1], Eva Lindgren[1], Elisabet Stener-Victorin[1*], Qiaolin Deng[1,2*]

[1] Department of Physiology and Pharmacology, Karolinska Institutet, Stockholm, Sweden
[2] Center for molecular medicine, Karolinska University Hospital, Stockholm, Sweden

[3] shared first authors; * corresponding authors

Corresponding authors

Qiaolin Deng
Department of Physiology and Pharmacology
Karolinska Institutet, Biomedicum B5
Center for molecular medicine, Karolinska University Hospital
171 77 Stockholm, Sweden
E-mail: qiaolin.deng@ki.se

Elisabet Stener-Victorin
Department of Physiology and Pharmacology
Karolinska Institutet, Biomedicum B5
171 77 Stockholm, Sweden
E-mail: elisabet.stener-victorin@ki.se

ORCID ID : Yu Pei 0000-0002-6219-3587; Sanjiv Risal, 0000-0003-1723-543; Hong Jiang, 0000-0002-8106-457X ; Haojiang Lu, 0000-0001-9051-0140; Qiaolin Deng, 0000-0001-5934-7816; Elisabet Stener-Victorin, 0000-0002-3424-1502

Abstract

Excessive androgen production and obesity are key to Polycystic ovary syndrome (PCOS) pathogenesis. PCOS-like mouse models induced by androgen exposure include the prenatal androgenized (PNA), peripubertal androgenized, and overexpression of nerve growth factor in theca cells (17NF), as well as the effect of diet-induced maternal obesity model on offspring. To reveal the molecular features of these models, we performed transcriptomic profiling of the hypothalamus, adipose tissue, ovary, and MII oocytes. The largest number of differentially expressed genes (DEGs) were found in the ovaries of 17NF and in the adipose tissues of peripubertal androgenized models. In contrast, the hypothalamus is most affected in PNA and maternal obesity models suggesting fetal programming effects. The Ms4a6e gene, membrane-spanning 4-domains subfamily A member 6E, a DEG identified in the adipose tissue in all PCOS-like mouse models is also differently expressed in adipose tissue of women with PCOS women, highlighting a conservative disease mechanism. Our comprehensive transcriptomic mapping of key target tissues of the PCOS pathology provides a unique resource when investigating molecular mechanisms induced by androgen exposure and highlights that there are critical windows for androgen administration and maternal obesity.

Significance statement

To model PCOS pathogenesis such as androgen excess, several mouse models have been developed to study pathophysiology. However, comprehensive transcriptomic profiling at the molecular level across key reproductive and metabolic tissues among different mouse models is still lacking. As each model could only mimic certain pathophysiological features, it is important to understand how the same target tissue is affected among different models. Hereby, we performed extensive transcriptomic profiling and comparison on the hypothalamus, adipose tissue, ovary, and MII oocytes in four frequently used PCOS mouse models. Our findings revealed that the hypothalamus is susceptible to fetal programming while adipose and ovary are more affected upon postnatal androgen exposure. Meanwhile, MII oocytes are variably affected by crosstalk with somatic tissues.

Introduction

Polycystic ovary syndrome (PCOS) affects around 15% of women in their reproductive age and the key feature of the syndrome is hyperandrogenism leading to abnormal follicular development, infertility, and an increased risk of type 2 diabetes (Kakoly et al., 2018; March et al., 2010; McCartney and Marshall, 2016; Stener-Victorin et al., 2020; Teede et al., 2018). There is a strong inheritance and genome-wide association studies (GWAS) reveal around 20 PCOS risk genes, but these account for less than 10% of the heritability (Dapas and Dunaif, 2020; Dapas et al., 2020; Day et al., 2018; Ruth et al., 2020; Shi et al., 2012; Stener-Victorin et al., 2020). It is now generally recognized that the etiology of PCOS is an interplay of genetic, epigenetic, and developmental factors (Dapas and Dunaif, 2022b; Dunaif, 2016; Escobar-Morreale, 2018; Risal et al., 2019; Stener-Victorin and Deng, 2021). To understand the complex pathophysiology of PCOS, more than 30 PCOS-like animal models have been developed to mimic certain pathophysiological features, among which rodent models (mice and rats) are the most common. Rodents and humans share evolutionarily conserved similarities in the regulation of reproductive function by the hypothalamic-pituitary-gonad (HPG) axis and ovarian folliculogenesis (Walters et al., 2012). Additionally, rodent models of PCOS can model many characteristics of the human disorder including hyperandrogenism, elevated LH, disrupted cyclicity, presence of follicular cysts/polycystic ovaries, and altered insulin sensitivity (Stener-Victorin et al., 2020).

Hyperandrogenism play a key role in the pathogenesis of PCOS and several PCOS-like mouse models have been created through androgen exposure at different developmental time points including the prenatal androgen (PNA) and the peripubertal androgen exposure models, as well as the transgenic17NF model overexpressing nerve growth factor (NGF) in the ovarian theca cells, all used in our labs (Caldwell et al., 2014; Dissen et al., 2009; Manti et al., 2018a; Manti et al., 2020; Risal et al., 2019; Wilson et al., 2014). These models differ in terms of the timing, dose, and androgen exposure approach that may result in different effects in downstream pathogenesis. So far, not much is known about the common and unique molecular features in major target tissues among these PCOS-like mouse models. Thus, the overall goal of this study is to define the molecular effects of fetal and adult programming by androgen in different PCOS-like mouse models as well as of maternal obesity model.

We studied the PNA model and the diet-induced maternal obesity model, the peripubertal androgenized model and the 17NF mice models, and performed single-cell RNA-seq of MII oocytes and bulk RNA-seq of target tissues including hypothalamus, subcutaneous adipose tissue, and ovary, being the most affected targets among all PCOS-like models, to characterize androgen- and obesity-specific molecular effects.

Results

Phenotypic features and experimental outline.

The PNA mouse model is established by dihydrotestosterone (DHT) exposure to the pregnant dam at gestational days 16.5–18.5 and the female first-generation offspring exhibits disturbed estrous cycle with elevated testosterone and LH levels and metabolic alterations in adulthood due to fetal programming of HPG axis (Manti et al., 2020; Moore et al., 2015; Sullivan and Moenter, 2004). The peripubertal androgenized mouse model induced by continuous DHT exposure from 4 weeks of age through a slow releasing DHT pellet or silastic tube implanted subcutaneously displays robust reproductive and cardiometabolic features reflecting PCOS symptoms (Caldwell et al., 2014; Manti et al., 2019b; van Houten et al., 2012). The genetically modified 17NF model overexpresses NGF in theca cells driven by 17α-hydroxylase promoter leading to ovarian hyperandrogenism (Dissen et al., 2009; Wilson et al., 2014). Similarly, it has

been reported that women with PCOS have a 2-fold increase in NGF in the ovarian follicular fluid compared to their control (Dissen et al., 2009) indicating the role of NGF in the PCOS pathology. In mice, excess ovarian NGF causes irregular cyclicity, compromised fertility, enhanced ovarian sex steroid production, and elevated granulosa cell apoptosis (Dissen et al., 2009). Moreover, these transgenic mice also display mildly elevated LH levels with increased testosterone production and metabolic dysfunction as reflected by impaired glucose metabolism and energy metabolism, aberrant adipose tissue morphology and function, and hepatic steatosis (Dissen et al., 2009; Manti et al., 2020; Wilson et al., 2014) mirroring the PCOS pathophysiology. Thus, these three PCOS-like mouse models are exposed to androgen at different developmental windows and serve our goal to delineate the shared or different molecular pathways/mechanisms and their contribution to reproductive and metabolic phenotypes of PCOS regulated by the HPG axis.

PCOS is also tightly linked with obesity, which is one of the important factors contributing to the development of PCOS. A large-scale genome-wide meta-analysis of women with PCOS demonstrates that there is a shared genetic architecture between metabolic traits, including obesity and PCOS (Day et al., 2018; Liu et al., 2022). Obesity is a common metabolic derangement in the PNA, peripubertal androgenized, and 17NF mouse models and there is evidence showing that the maternal obesity model also affects female germ cells and their female offspring (Han et al., 2018; Risal et al., 2019; Saben et al., 2016). Therefore, we also include the diet-induced maternal obesity model to compare the effects of diet-induced obesity with that of androgen-induced programming in target tissues and oocytes in first-generation female offspring.

The phenotypic features of the PNA and the maternal obesity, representing fetal programming, and the peripubertal androgenization and17NF representing adult programming mouse models are summarized in **Fig. 1a** (Caldwell et al., 2014; Dissen et al., 2009; Manti et al., 2018a; Manti et al., 2020; Risal et al., 2019; Wilson et al., 2014). To understand and define the common and distinct molecular signatures of key targe tissues in these mouse models, we carried out bulk mRNA sequencing of the hypothalamus, subcutaneous adipose tissue, and ovary as well as single-cell mRNA sequencing of MII oocytes using Smart-seq2 (**Fig 1b-e**).

Unique transcriptomic profile of hypothalamus induced by fetal and adult androgen exposure.

Differentially expressed genes (DEGs) in the hypothalamus, the neural control center for the endocrine and reproductive systems, within PNA, peripubertal androgenized, and 17NF models together with fetal exposure to maternal obesity are given in **Supplementary Table S1**. There are five overlapping DEGs between the PNA and maternal obesity mouse models: *Cfd*, *Cyp11a1*, *Fabp4*, and *Hsd3b1,* in addition to *Scd1* which is also differently expressed in the 17NF model (**Fig. 2a**). There are no common DEGs in the peripubertal androgenized and the 17NF mouse models (**Fig. 2a**). Moreover, there are three common DEGs, *Nudt3, Inha,* and *Mapk8ip3*, between PNA and the peripubertal androgenized model and one additional DEG (*Rps25*) between PNA and 17NF models (**Fig.2a**). To further annotate the function of identified DEGs in the hypothalamus across these four animal models, we performed GO enrichment biological processes analysis. Interestingly, all animal models showed enriched pathways related to lipid, nucleic acids, carbohydrate, nucleotide, and steroid hormone metabolism, but these pathways were regulated by different sets of genes (**Fig. 2b).** In addition, gonad development GO terms are found in the PNA and the peripubertal androgenized mice which likely reflects the unique effect of systematic androgen exposure on the hypothalamus-ovary axis related to reproduction dysfunction (**Fig. 2b**). Notably, common biological pathways were found between the PNA, maternal obesity, and peripubertal androgenized models whereas the 17NF model deviated, suggesting that different molecular mechanisms. All DEGs involved in

lipid metabolism, steroid metabolism, and gonad development biological processes were further highlighted in their gene expression in each model with a color corresponding to each pathway highlighted (**Fig. 2c-f** and **Supplementary Table S2)**. Most genes in these pathways were upregulated in the PNA model whereas most genes were downregulated in maternal obesity, indicating opposite effect on the hypothalamus in the fetal programming by androgen and diet, respectively differentially expressed genes (DEGs) (**Fig. 2c and 2d**). Notably, DEGs are different in each model although involved in the same biological processes. For example, in the hypothalamus of the PNA mouse model, *Acsbg1*, *Cd74*, *Akr1cl*, *Fabp4*, and *Scd1* are DEGs involved in fatty acid biosynthesis and steroid metabolism (**Fig. 2c**) whereas in the peripubertal androgenized model are *Atp5j*, *Gal,* and *Inha* differentially expressed in the same pathways (**Fig. 2e**). In the 17NF hypothalamus, a panel of DEGs e.g., *Acot7, Elovl6, Fasn, Hmgcs1,* and *Scd1* (**Fig. 2f**) are involved in triglycerides and cholesterol metabolism. The implicated function of selected DEGs has been further illustrated in the lipid and steroid metabolism pathways (**Fig. 2g**).

Fetal and adult androgen exposure revealed different transcriptomic profiles in the ovary. One of the hallmarks of PCOS is chronic anovulation and the ovaries of women with PCOS contain more small antral follicles than normal ovaries. The irregular estrous cycle is one of the most prominent phenotypes in these PCOS-like mouse models. To further explore the underlying transcriptomic change that might be leading to the ovarian phenotypes, we first conducted DEGs analysis in the ovary among the PCOS-like models and the maternal obesity model (**Fig. 3a,** and **Supplementary Table S3**). The greatest number of DEGs is found in the peripubertal androgenized model coinciding with a strong reproductive phenotype induced by adult programming of androgen. We find 16 common DEGs among the three PCOS-like models and 1 DEG (*Heph*) shared by all four models. To compare the common and unique pathways influenced by fetal and adult programming, we did a GO enrichment analysis of biological processes on DEGs (**Supplementary Table S4**) in all four animal models. We identified pathways involved in metabolism, glucose homeostasis, steroid hormone metabolic process, response to insulin, and gonad development (**Fig. 3b**). The common pathway among the three PCOS-like models is the ERK1 and ERK2 cascade. The ovarian follicle development pathway is shared between PNA and peripubertal androgenized models in agreement with the effects of DHT exposure. Notably, the unique pathway in PNA is placenta development, which reflects PNA modeling strategy, and maternal behavior in the peripubertal androgenized mouse model, which is in line with our previous observations that PNA and peripubertal androgen exposure induce anxiety-like behavior (Risal et al., 2021).

To understand how time point and dose of androgen and diet exposure affects the ovarian gene expression profile in these mouse models, we examined all DEGs that are involved in ovulation and identified several common and unique genes (**Fig. 3c**). *Bmpr1b* and *Fshr* are downregulated in PNA but upregulated in the peripubertal androgenized model indicating that the window of androgen exposure is critical and results in a different outcome in the ovulation cycle. The *Esr2* expression, on the other hand, is downregulated in both PNA and peripubertal androgenized mice. *Esr2* mediated signaling is predominant in ovarian granulosa cells and plays an important role in follicle maturation and ovulation (Khristi et al., 2018). PNA and maternal obesity models, representing fetal programming, shared two downregulated genes *Bmpr1b* and *Esr2,* and *Inha* is upregulated in the peripubertal androgenized and in the17NF models, respectively. Different ovarian steroid hormones are involved in regulating timely ovulation in female mammals. We found that the steroid hormone biosynthesis is also affected in the PNA, in the peripubertal androgenized and in the diet-induced obesity models (**Fig. 3c**). In the PNA and maternal obesity models, respectively, *Hsd11b2* is commonly downregulated and in the

peripubertal androgenized and 17NF models are *Hsd17b7*, *Hsd3b1*, *Hsd3b2, Hsd3b6*, *Hsd17b7*, *Hsd3b1*, and *Hsd11b2* dysregulated.

To further explore the androgen exposure effects, we compared the DEGs with genes linked to PCOS SNPs identified in Genome-Wide Association Studies (GWAS) studies. We found that seven PCOS risk genes were dysregulated in our animal models (**Fig. 3d**). The reproductive risk genes (*Fshr* and *Lhcgr*) are downregulated in the PNA model, and the metabolic risk genes (*Insr* and *Rad50*) are downregulated in the maternal obesity model. While the peripubertal androgenized model have both metabolic and reproductive risk genes upregulated (*Amh*, *Amhr2*, *Fshr*, and *Rab5b*), and in the 17NF model is *Amh* is downregulated (**Fig. 3d**). These findings support the relevance of the different PCOS-like models reflecting common PCOS-related ovarian cellular processes.

To find common gene sets signature across PCOS-like mouse models, we conducted a weighted gene co-expression network analysis (WGCNA) to define the relationship between gene sets (modules) and phenotype features (Langfelder and Horvath, 2008). We identified 16 significant gene modules (**Fig. 3e** and **Supplementary Table S5**) and module1 (MEblack) contains 215 genes that were expressed across the PNA, peripubertal androgenized, and 17NF models, respectively, but not in the maternal obesity model. Gene network analyses of the 215 genes in the MEblack module revealed the androgen receptor and its interactome are preserved across the three PCOS-like mouse models, but not in the obesity model. The low-density lipoprotein receptor (LDLR) mRNA binding and splicing proteins encoded by *Sf1, Fubp1,* and *Fubp1* are also preserved in this module (**Fig. 3f, Supplementary Fig. S1a,** and **Table S5**).

Fetal and adult androgen exposure modulates ligand-receptor interaction in MII oocytes and ovary.

To further understand how different windows of androgen and maternal obesity exposures affect the development and gene expression of MII oocytes, we carried out the single-cell transcriptomic analysis of MII oocytes from the four animal models. Unique and overlapped genes are presented in the Venn diagram (**Fig. 4a** and **Supplementary Table S6**). Interestingly, most DEGs were detected in the MII oocytes of the 17NF model suggesting that genetic modification of granulosa cells greatly affects the oocytes. In addition, we found 34 common DEGs among the three PCOS-like models and 10 DEGs (*Obox5, Tcl1b1, Mki67, Rapgef5, Mphosph6, Afap1l2, Gmnn, Mfap1b, Gadd45gip1, Ints9*) are shared by all four models. To define the functional role of these DEGs, GO annotation revealed common biological processes involved in all models such as glucose metabolic process, response to insulin, meiotic cell cycle, etc. One pathway i.e., development of primary sexual characteristics was shared by the three PCOS-like mouse models. And 17NF models contained several unique pathways such as ovarian follicle formation, steroid hormones, and ERBB signaling pathways, suggesting strong effects of local increase in androgen due to genetic modification of granulosa cells (**Fig. 4b)**. Several DEGs in MII oocytes in each model were also linked to PCOS susceptible gene loci identified from GWAS (**Fig. 4c)**. We found that 17NF showed the most common DEGS with PCOS GWAS genes compared to other models. As there is plentiful evidence to show that androgens stimulate the growth of both preantral and antral follicles and impairs the follicle maturation (Nisenblat and Norman, 2009), and as MII oocytes and surrounding follicular niche cells communicate bi-directionally in the ovary, we further investigate ligand-receptor interactions between MII oocytes and ovaries by using a ligand-receptor database (CellChat DB) (Jin et al., 2021).

By ligand-receptor analysis, we identified several differential signaling pathways in each animal model. The members of BMP signaling have been reported strongly related to follicular development and involved in PCOS pathology (Magro-Lopez and Muñoz-Fernández, 2021). In

the PNA, maternal obesity, and the 17NF models, respectively, we found that BMP signaling is reduced compared to control (**Fig. 4d-g**): the ligand Bmp4 and its receptors [Bmpr1a+Bmpr1b+Bmpr2] in PNA; Bmp7 [Bmpr1a+Bmpr1b+Bmpr2] in maternal obesity; Bmp5+Bmp15 [Bmpr1b+Bmpr1a] in 17NF model, respectively. Interestingly, AMH signaling is reduced in PNA and maternal obesity models (**Fig. 4d and e**). This reduction is likely due to androgen induced reduction of oocyte-specific BMP which normally stimulate AMH levels. We found several cell proliferation signaling pathways such as EGF signaling: Tgfa [Egfr+Erbb4], IGF signaling: Igf1 [Igfr+Itga6] to be increased in the peripubertal in line with previous studies (Franks and Hardy, 2018). KIT signaling involved in the regulation of follicle growth and oocytes development is increased in PNA, peripubertal androgenized model and in 17NF models, respectively. Notably, we found activation of inflammatory pathway including TRAIL: Tnfs10 [Tnfrs10b]; CSF: Il34 [Csfr and Csf1-Csfr1]; LIFR: Ctf [Lifr] in all models. In the PNA model we found increased enrichment of ligand-receptor pairs that are potentially driven by *in utero* androgen exposure. Specifically, activin: *Inhba* [Acvr1b+Acvr2a], adiponectin: Adipoq [Adipor2 and Adipor1], tumor necrosis factor-related apoptosis-inducing ligand (TRAIL) Tnfs10 [Tnfrs10b] and luteinizing hormone subunit beta (LHB) Lhb [Lhcgr] (**Fig. 4d).** In the peripubertal androgenized model, ligand-receptor pairs in CCL with Ccl25 [Ackr4], IL1 with Il1a [Il1r2] and Il1b [I1r2] and WNT (Wnt1 [Fzd1 to Fzd10 +Lrp5] pathways were enriched compared to control (**Fig. 4f)**. Notably, several more signaling pathways for ligand-receptor pairs were enriched in the 17NF model such as NRG [Erbb4-Nrg2), with GnRH [Gnrh1, Gnrhr] and GDF Gdf9 [bmpr2] uniquely found in 17NF model compared to control (**Fig. 4g).** Collectively, these results suggest that signaling pairs involved in immunity, development, and fertility are differently affected in each model.

Fetal and adult androgen exposure modulates metabolic pathways in MII oocytes

Emerging evidence indicates that metabolism is a major determinant of oocyte quality (Warzych and Lipinska, 2020). Besides the ligand receptor signaling effects, to investigate if any metabolic changes affect oocytes quality, we quantified the metabolism activity of MII oocytes in the PCOS-like models and in the maternal obesity model. Peptide hormone metabolism is affected in the PNA model (**Fig. 5a**). Several DEGs involved in this pathway such as *Foxo1, Atp2a2, Prkcb, Ctnnb1, Lpin1, Srsf3, Rac1* might be crucial to drive this pathway. *Foxo1* belongs to the forkhead transcription factor family known to involve cellular functions including cell growth and differentiation. The expression of *Foxo1* is highly increased in cumulus cells of women with PCOS. *Foxo1* is a key downstream molecule of IGF-1 signaling, regulating the circulatory metabolism and hormone levels in hypothalamus-pituitary axis and adipose tissue. Glucose is essential to generate ATP for energy in the metabolite cumulus-oocyte complex. Oocyte itself is poor to metabolize glucose, instead, the oocyte is reliant on cumulus cells to take up glucose on its behalf. In the maternal obesity model, the glucose metabolism is significant decreased, indicating delayed oocytes maturation in offspring of obese mothers (**Fig. 5b**). The DEGs involved in this pathway are *Arfgef1, Ogt, Ogdh* and *Actn3*. In the peripubertal androgenized model, metabolism is significantly reduced and the expression of DEGs involved in steroid pathway like *Yap1*, linked to PCOS susceptible gene loci identified from GWAS; *Sirt1* in regulation of systemic energy and steroid hormone homeostasis are also decreased (**Fig. 5c**). We also identified that the unique oxidative phosphorylation metabolism pathway is significantly upregulated in 17NF mice model (**Fig. 5d**).

Fetal and adult androgen exposure alters gene expression in adipose tissue.

Obesity is a common feature in women with PCOS and adipose tissue dysfunction is likely involved in the development of the syndrome and associated metabolic disturbances. All

models used have increased fat mass and enlarged adipocytes (**Fig. 1a)** indicating aberrant adipose tissue function and metabolic dysfunctions. Transcriptomic analysis of subcutaneous adipose tissue showed common and unique DEGs (**Fig. 6a** and **Supplementary Table S8)**. The largest number of DEGs (1910) was found in the peripubertal androgenized model suggesting potent adult programming of DHT in adipose tissue (**Fig 6a**). Total, 18 common DEGs were detected in the three PCOS-like models, whereof 8 were shared by all models. Subsequent functional analysis of DEGs in each model show shared biological processes; lipid, glucose, and nucleotide metabolism, regulation of inflammatory response, and response to testosterone, except in 17NF model (**Fig. 6b)**. Notably, adipose tissue development was enriched in peripubertal androgenized and 17NF models as adult programming models. We then selected DEGs in each model involved in the same pathways and show that in response to a steroid hormone, *Apoa1* and *Pon1* were both downregulated in PNA and maternal obesity models indicating a fetal programming effect, whereas *Hsd11b*, *Lep*, *Lipe*, and *Sqle* were affected in the peripubertal androgenized and 17NF models (**Fig. 6c**). Notably, *Pon1* was influenced by both fetal and adult androgen exposures and by maternal obesity in adipose tissue. However, *Pon1* expression is upregulated in PNA and peripubertal androgenized models whereas it was downregulated in 17NF and maternal obesity models. *Pon1* gene encodes the calcium-dependent antioxidant enzyme paraoxonase1. It has been shown that there is an inverse correlation between *Pon1* and hyperandrogenism due to PCOS (Dadachanji et al., 2015). As obesity is linked to chronic inflammation, we also analyzed the DEGs in the regulation of inflammatory response. *Ccr7*, a chemokine receptor expressed in various immune cells and is linked to obesity as its knockout in mice results in protection from diet-induced obesity (Sano et al., 2019). Upregulation of *Ccr7* in adipose tissue indicates inflammation due to increased adiposity (**Fig. 6c** and **Supplementary Table S9**). This notion is further supported by higher expression pattern of *Cd44* in the PNA and maternal obesity models. *Cd44* likely plays a regulatory role in obesity-linked metabolic syndrome (Kang et al., 2013). In peripubertal androgenized and 17NF models, the *Ido1,* an anti-inflammatory gene was down-regulated, and up-regulated respectively (**Fig. 6d** and **Supplementary Table S9**). In contrast to fetal programming (PNA and maternal obesity), only adult programming models (peripubertal androgen exposure and 17NF) showed distinct impaired glucose homeostasis (**Fig. 1a**). Our transcriptomic profile of adipose tissue showed that upregulated *Mup1* expression is common to PNA, maternal obesity, and peripubertal androgenization (**Supplementary Fig.S2**). The functional enrichment analyses in these models showed that *Mup1* is involved in glucose homeostasis an indicator of insulin sensitivity (Chen et al., 2015). In the 17NF model, functional enrichment of DEGs in the glucose homeostasis displayed upregulation of *Insr*, *Irs1*, *Ppara, Acacb, Dgal2, and Rorc* (**Supplementary Fig.S2**). Taken together, independent of a type and window of exposure to androgen or maternal obesity, our findings reveal that adipose tissue is largely affected likely contributing to aberrant adipose tissue function and glucose intolerance often observed in these models (**Fig. 6c)**. Next, we performed correlation analyses between fold changes of DEGs in each mouse model with published fold changes of DEGs in adipose tissue of women with PCOS (Divoux et al., 2022) and found strong correlation of DEGs between each model and women with PCOS (**Fig. 6d and Supplementary Table S10**). Interestingly, *Ms4a6e* is common to all PCOS-like mouse models also with a high fold change in expression in adipose tissue of women with PCOS (**Fig. 6d and Supplementary Table S10**), both fetal programming models, PNA and the maternal obesity, showed a strong correlation with *CCL22* expression in women with PCOS (**Figure 6d)**. This finding suggests that gene expression of subcutaneous adipose tissue in all mouse models recapitulates gene expression of women with PCOS.

Transcriptomic interaction among hypothalamus, ovary, adipose tissue, and MII oocytes in PCOS-like animal models and maternal obesity model.

Next, we explored the DEGs affected metabolic pathways including peptide hormone metabolism, steroid hormone metabolism and fatty acid metabolism among target tissues in each animal model for common and unique DEGs involved signaling pathways across all tissue in PCOS-like mouse models and maternal obesity model. (**Fig. 7a, Supplementary Table S11-13**). By ligand-receptor analyses, we identified possible signaling pathways such as BMP signaling pathway, Kit signaling pathway, adiponectin uniquely affected by PNA model, EGF and IGF (insulin signaling pathway) pathways affecting MII oocytes quality.

The ovary and adipose tissues shared many common DEGs among the PCOS-like mouse models indicating a potential transcriptional network modulated by hyperandrogenism in the peripheral tissues, with most DEGs in the peripubertal androgenized model followed by the 17NF and the PNA mouse models as listed in **Supplementary Table S11**. Interestingly, as a fetal programming effect first generation female offspring in the maternal obesity model had more common dysregulated genes in the ovary and adipose tissue compared to the offspring in the PNA model. Several genes in the PNA, peripubertal androgenized, and 17NF models established a regulatory network in the hypothalamus-ovary-adipose axis with either the same or family member genes. For example, in the PNA model, *Atp1b1* and *Atp2a3* are downregulated in the hypothalamus and adipose tissue, respectively, showing family members in the transcriptomic network. To extend exploration, we consider a panel of genes in steroid hormone metabolism regulation. The *Hsd3b1* expression is affected by androgen and maternal obesity in the fetal programming milieu. In the PNA model, *Hsd3b1* is upregulated in the hypothalamus and MII oocytes, whereas in maternal obesity *Hsd3b1* is downregulated in the hypothalamus and upregulated MII oocytes (**Fig. 7a and Supplementary Table S12**). On the other hand, adult programming displayed a consistent pattern of gene expression as shown in the peripubertal androgenized and 17NF models. Besides common gene signatures in different tissues of PCOS-like mouse models, we demonstrated a unique gene influenced by fetal and adult programming resulting from hyperandrogenism and maternal obesity exposure with down-regulated expression of *Cfd*, which is not affected in peripubertal androgenized and 17NF models. Additionally, in the PNA model, *Fabp4* is downregulated in the hypothalamus and upregulated in the ovary, and *Fabp3* (family member match of *Fabp4*) is upregulated in adipose tissue, indicating an influence of prenatal androgenization on lipid metabolism in different tissues. Adult programming models also showed a unique differential gene expression pattern of *Car3*, *Cyp27a1*, *Car5b*, and *Cyp2d22* in the ovary and adipose tissue (**Fig. 7a and Supplementary Table S13**).

Discussion

PCOS is a heterogeneous disorder involving a complex interaction between metabolic and reproductive pathways. This syndrome is characterized by persistent anovulation, oligomenorrhea or amenorrhea, and hyperandrogenism, excluding other conditions causing such symptoms. Although there are several well-characterized mouse models phenocopying PCOS features and maternal obesity, none of these models have been in-depth transcriptomic profiled. Therefore, we took the opportunity to perform such profiling of three key targets tissues as well as in MII oocytes with the overarching objective to define the molecular effects of fetal and adult programming by androgen in different PCOS-like mouse models as well as the effects of maternal obesity.

Like other complex diseases such as type 2 diabetes (Chen et al., 2021; Flannick and Florez, 2016), PCOS is a highly heritable disorder. However, only a small proportion of the heritability can be accounted for by the ~20 susceptibility loci identified by GWAS (Dapas and Dunaif, 2022a). Nonetheless, reproductive and metabolic phenotypes are associated with specific PCOS susceptibility loci, supporting the role of genetic factors in pathogenesis (Dapas and Dunaif,

2022a). Indeed we recently showed that ~70% of a daughter of women with PCOS receive the diagnosis of PCOS around their twenties (Risal et al., 2019). Moreover, we also showed that transmission of PCOS across generations in mice occurs as a result of maternal androgen exposure implying that the maternal-fetal environment may account for the mother-to-daughter inheritance of the syndrome in a non-genetic manner (Risal et al., 2019). Clinical evidence of a hyperandrogenic fetal environment is that PCOS women's daughters display a longer anogenital distance (Barrett et al., 2018) and higher levels of facial sebum production (Homburg et al., 2017) at birth, markers of *in utero* hyperandrogenism. Amniotic fluid from daughters of women with PCOS showed significantly elevated testosterone compared with control women during mid-gestation (Palomba et al., 2012), which represents a critical window for the development of the hypothalamus. Exposure to elevated level of androgen might result in fetal programming of the germ cells, hypothalamus, and other targeted tissues.

The adipocyte-fatty-acid-binding protein (FABP4) is an adipokine involved in the regulation of whole-body insulin sensitivity, as well as lipid and glucose metabolism, and has been implicated in the development of PCOS through regulation of transcription and/or protein alterations (Wang et al., 2009). These previous reports support our findings that the *Fabp4* gene expression is dysregualted in the hypothalamus only in our fetal programming mouse models (PNA and diet-induced maternal obesity), but not in the adult programming models (peripubertal androgenization and 17NF). In the peripubertal androgenization mice, but not in the fetal programming models, the expression of *Gal* is downregulated in the hypothalamus, which codes neuropeptide galanin. Serum level of galanin has been implicated as a risk factor in metabolic and cardiovascular diseases in women with PCOS (Altinkaya, 2021). The expression of *Acot7, Elovl6, Fasn, Hmgcs1,* and *Scd1* genes involved in triglycerides and cholesterol metabolism and display differential expression patterns and are upregulated in the PNA and 17NF models and downregulated in maternal obesity mouse model in line with previous observations (Wang et al., 2009).

Interestingly, the strongest GO enrichment pathways in the hypothalamus were found in the PNA and maternal obesity models followed by peripubertal androgenized with the least enrichment in 17NF mouse models indicating that the fetal programming exerts a stronger effect on the brain compared to adult programming. That adult programming has less pronounced effect on hypothalamic gene expression is supported by the recent finding that peripubertal androgen exposure does not impact luteinizing hormone pulse frequency (Coyle et al., 2022) as it does in the PNA model (Moore et al., 2015; Sullivan and Moenter, 2004). Thus, the discrepancies in the hypothalamic transcriptomic and functional enrichment profiling among the mouse models suggest there are critical windows for exposure of androgens and obesity that affect the development of hypothalamus. The hypothalamic neurogenesis occurs between E10.5 and E16.5 in mice followed by gliogenesis and terminal differentiation which overlaps with the sexual maturation of the animal (Shimogori et al., 2010). The different time points of androgens exposure affect distinct stages of hypothalamus development. Hypothalamus also regulates the reproductive axis and both PNA and peripubertal androgenized mouse models showed GO annotation linked to gonad development.

To extend our findings in the hypothalamus to the reproductive axis in these animal models, we performed transcriptomic analyses also of the ovaries and MII oocytes from these models. The ovary is a heterogeneous organ and comprises different cell types. For functional reproductive life, both autocrine and paracrine communications among these cells play an important role in follicle growth and oocyte maturation. To understand the temporal influence of androgen in fetal and adult programming, we analyzed ligand-receptor interaction between the ovary and

MII oocytes in these PCOS-like animal models. Our study showed common and unique ligand-receptor interaction in ovary-MII oocytes in fetal (PNA and maternal obesity) and adult programming PCOS-like models. The 17NF model, a transgenic model with selective overexpression of nerve growth factor in the ovarian theca-interstitial cells, directly influence follicular development displays unique differential ligand-receptor pairs such as GDF (Gdf9-bmpr2). Gdf9 is an oocyte-specific gene, playing an important role in oogenesis (Gilchrist et al., 2008). Moreover, we identified the differential signaling pathways such as BMP signaling affecting follicle development; EGF and IGF signaling affects cell proliferation; KIT signaling that is import for oocyte maturation in fetal and adult programming PCOS-like mice models; adiponectin signaling as a positive regulator of metabolic function (Li et al., 2020). Our ligand-receptor interaction analysis provides a resource to study the signaling changes in the ovary. Notably, we identified the biological processes that are involved in metabolic pathways in MII oocytes in all PCOS-like mice models and in the maternal obesity mice model.

It has been reported that hypothalamic *Gmp6a*, *Rgs2, and Txnip* are likely to be involved in an estrous cycle in female mice (Knoedler et al., 2022). Moreover, *Rgs2* is regulated by GnRH (Wurmbach et al., 2001), which implies the hypothalamus-ovary axis in the regulation of estrous cyclicity. In support of these previous findings, we found that *Gpm6a* expression is downregulated in the PNA model, and *Txnip* and *Rgs 2* are upregulated in the hypothalamus with the latter also detected by WGCNA analysis in the ovary supporting the strong link between hypothalamus-ovary axis in the regulation of estrous cyclicity. Peripubertal androgenization also affects the estrous cycle gene expression with downregulation of *Gal* in the hypothalamus (Knoedler et al., 2022). These findings support that *Gmp6a*, *Rgs2, Txnip,* and *Gal* dysregulation is linked to irregular estrous cycle in the PNA and peripubertal androgenized mouse models. Moreover, functional analysis showed similar activated pathways among the four models. Our in-depth assessments of DEGs related to estrus cyclicity revealed that the fetal programming, as in PNA and diet-induced obesity, showed a distinct and common expression pattern compared to those influenced by adult programming. Additionally, activated ovarian pathways linked to the placenta development (*E2f8, Fgfr2, Cited2, Cdh1, Krt19, Socs3*) in PNA and maternal behavior (*Oxtr, Kalrn, Crebrf,* and *Pten*) in peripubertal androgenized mice are unique considering the temporal difference in androgen exposure.

The function of subcutaneous fat is coordinated by neuroendocrine and hormonal cues from outside of the fat depot (Priest and Tontonoz, 2019). Moreover, hyperandrogenism affects adiposity and adipogenesis. Subcutaneous adipose tissue transcriptomic profiling displayed dysregulated *Pon1* expression and is affected by exposure to hyperandrogenism in fetal and adult life as well as exposure to maternal obesity. It has been shown that dyslipidemia in women with PCOS is linked to PON1, an oxidative enzyme associated with apoA1 on HDL particles (Perovic Blagojevic et al., 2021). In line with this observation, all PCOS-like mouse models and the maternal obesity model shared GO enrichment related to response to oxidative stress: in PNA and maternal obesity and peripubertal androgenized and 17NF. To link our preclinical findings in adipose tissue to humans, we overlapped adipose tissue DEGs in the different mice models and with adipose tissue DEGs of women with PCOS (Divoux et al., 2022). The result showed that altered *MS4A6E* gene expression is shared by all PCOS-like models, a gene that has been shown to be involved in neurodegenerative disorders (Harwood et al., 2021) . Moreover, we found that adult androgen programming has highest number of common DEGs between the ovary and adipose tissue with the lowest number of common DEGs in maternal obesity followed by PNA mouse models. Common gene regulation between the hypothalamus, ovary, and adipose tissue was found in PNA (*Ccl* members), peripubertal androgenized (*Wfdc* members), and 17NF (*Elovl* members).

Our study provides a comprehensive transcriptomic profiling of key target tissues in three mouse models of PCOS and one of maternal obesity and is a unique resource for the research community. Several common functional pathways are identified among all mouse models despite different gene targets. The peripheral tissues: ovary and adipose tissue are more affected than the hypothalamus in the peripubertal androgenized, the 17NF, and in the maternal obesity mouse models. Not surprisingly, the fetal programming exerts a strong effect on hypothalamic gene expression as compared to the peripubertal and adult programming, and the transgenic 17NF mouse model exerted the strongest effect on ovarian gene expression profile. The adipose tissue of the peripubertal androgenized model was the most affected which is in line with the phenotype of this model with increased fat mass and altered glucose metabolism. Importantly, the increased/decreased *MS4A6E* expression in subcutaneous adipose tissue of women with PCOS and all mouse model, highlights a conservative disease mechanism.

Methods

Ethical Approvals: All animal experiments were approved by the Stockholm Ethical Committee for Animal Research (10798-2017 and 17538-2020) in accordance with the legal requirements of the European Community (SJVFS 2017:40) and the directive 2010/63/EU of the European Parliament on the protection of animals used for scientific purposes. Animal care and procedures were performed in accordance with guidelines specified by European Council Directive and controlled by Comparative Medicine Biomedicum, Karolinska Institutet, Stockholm, Sweden.

Experimental animals: All mice were maintained under a 12-h light/dark cycle and in a temperature-controlled room with *ad libitum* access to water and a diet. Prior to starting the experiments, the number of animals required for the experiments was estimated from our previous work based on the same model where the success of the breeding was about 60% of the F0 dams (Fornes et al., 2019; Manti et al., 2019a; Manti et al., 2018b; Risal et al., 2019).

Prenatal androgen exposed model: To generate prenatal androgen exposed offspring (Risal et al., 2019), 3-week-old female C57Bl/6J mice (Janvier Labs, Le Genest-Saint-Isle, France) were fed on control diet (Research Diets, D12328) comprising 11% fat, 73% carbohydrates [0% sucrose], and 16% proteins. These mice were randomly divided into the control and PNA groups after mating with male mice fed on chow diet and were subcutaneously injected from E16.5 to E18.5 with 50 µl of a solution containing **1)** a mixture of 5 µl benzyl benzoate (B6630; Sigma-Aldrich) and 45 µl sesame oil (S3547; Sigma-Aldrich, St. Louis, Missouri, USA) i.e. vehicle (control), or **2)** 250 µg dihydrotestosterone (5α androstan-17β-ol-3-one, A8380; Sigma-Aldrich, St. Louis, Missouri, USA) dissolved in a mixture of 5 µl benzyl benzoate and 45 µl sesame oil. First generation female offspring were subjected to phenotypic testing prior finalization which has been described in detail elsewhere (Risal et al., 2019).

Peripubertal DHT exposed model: To generate hyperandrogenemic females, 4-week-old adult female mice C57Bl/6J mice (Janvier Labs, Le Genest-Saint-Isle, France) were implanted subcutaneously with a 10-mm length (pellet) of DHT or, as control, a no-DHT pellet (Wang et al., 2018). This 10-mm pellet contained 5.24 mg DHT. Before implantation, the pellets were equilibrated in saline for 24 hours at 37°C (Wang et al., 2018). DHT pellets were prepared as described (Au - Xue et al., 2018).

17NF mouse model: The breeding, genetic background, and the generation of the transgenic 17NF mice (MGI Cat# 5662267, RRID: MGI:5662267) has previously described in detail (Dissen et al., 2009; Manti et al., 2020). These mice overexpressed NGF driven by the 17alpha-hydroxylase gene promoter in theca cells of the ovary. The transgene expression in each batch of homozygous 17NF mice was confirmed by genotyping.

Diet-induced maternal obesity model: To generate the diet-induced maternal obesity model, 4-week-old female C57Bl/6J mice (Janvier Labs, Le Genest-Saint-Isle, France) were fed a HFHS diet (Research Diets, D12331) comprising 58% fat, 26% carbohydrates [17% sucrose], and 16% proteins or a control diet (Research Diets, D12328) for 6 weeks prior mating (Risal et al., 2019). Eight- to twelve-week-old male mice fed on chow diet were used for mating and fed an in-house chow diet (*R34,* Lantmännen, Kimstad, Sweden). First generation female offspring were subjected to phenotypic testing which has been described in detail elsewhere (Risal et al., 2019).

MII oocytes and tissues collection: To collect MII oocytes from PNA, peripubertal DHT, 17NF, and maternal obesity mouse models, 20-week-old female were superovulated by

injecting 5 IU of pregnant mare's serum gonadotropin (PMSG) (Folligon, MSD Animal Health Care, Stockholm, Sweden) followed by 5 IU of human chorionic gonadotropin (hCG) (Pregnyl 5000IE, Merck Sharp & Dohme AB, Stockholm, Sweden) 48 h after PMSG priming. Cumulus-oocyte complexes were isolated at 16 h post-hCG injection from oviduct ampulla. Denuded single MII oocytes were then obtained by removing the cumulus mass in M2 medium (M7167; Merck KGaA, Darmstadt, Germany) containing 0.3 mg/ml hyaluronidase (H3884; Merck KGaA, Darmstadt, Germany) at room temperature.

At finalization, mice were fasted for 2 hours before blood, oocyte, and tissue collection. Briefly, the subcutaneous adipose tissue, ovaries, and hypothalamus were quickly dissected on ice, snap frozen in liquid nitrogen, and stored at −80°C.

RNA isolation and Bulk RNA sequencing library preparation: Mouse subcutaneous adipose tissue, hypothalamus and ovary were homogenized in 1ml TRI reagent (T9424, Sigma-Aldrich). Total RNA was extracted as per the manufacturer's instructions and 1ng of total RNA was applied to bulk RNA sequencing library. Sequencing libraries were generated according to Smart-seq3 protocol (Hagemann-Jensen et al., 2020). Briefly, polyA(+) RNA was reverse transcribed by Maxima H-minus reverse transcriptase (Thermo Fisher). The second strand synthesis was conducted by a template-switching reaction and 12 cycle of PCR was performed for cDNA amplification by KAPA HIFI Hot-Start polymerase (Roche). Then cDNA was purified by 22% PEG (Sigma Aldrich) beads. Aglient 2100 BioAnalyzer (Agilent Technologies) was performed to check the quality and quantity of cDNA libraries. Sequencing libraries were generated by tagmenting 200 pg cDNA using Nextera XT Tn5 transposase (Illumina) and amplified for 10 cycles.

MII oocytes from 17NF model sequencing library preparation: Single- MII oocyte was prepared by Smart-seq2 protocol. Following cell lysis, polyA(+) RNA was captured by SuperScript II reverse transcriptase (Thermo Fisher), Template swishing reaction was utilizing for second-strand synthesis. cDNA amplification was prepared by 14 cycles of PCR reaction using KAPA HIFI HotStart ReadyMix (KAPA Biosystems) and the libraries were purified by magnetic beads. Aglient 2100 BioAnalyzer (Agilent Technologies) were applied for checking the cDNA quality. Sequencing libraries were generated by tagmentation 1ng cDNA by Tn5 transposase and amplified for 8 cycles.

MII oocytes from Peripubertal model sequencing library preparation: Single-MII oocytes was prepared by Smart-seq3 protocol. Following cell lysis, polyA(+) RNA was reverse transcribed by Maxima H-minus reverse transcriptase (Thermo Fisher) as mentioned below. cDNA amplification was performed by PCR (14 cycles) followed by beads purification. Sequencing libraries were generated by Nextera XT Tn5 transposase (Illumina) and amplified for 10 cycles.

RNA-seq data processing: Raw reads generated by Smart-seq3 protocol were mapped by zUMIs pipeline (Parekh et al., 2018). Raw reads generated by Smart-seq2 protocol were mapped to mouse reference genome (GRCm38/mm10) using STAR default arguments.

DEG analysis and Gene Ontology analysis: DEGs were calculated using DESeq2 method (R package "DEGseq2 of version 1.34.0). DEG genes were defined by $p < 0.05$ with log2 foldchange > 0.5 or log2 foldchange < -0.5. Gene Ontology analysis of DEGs was performed by 'Clusterprofiler' R package.

WGCNA analyses: Normalized data were performed by 'WGCNA' R package. The power parameter with soft threshold of 9 was selected by 'pickSoftThreshold' function. The Pearson correlation was used in the analyses and the correlation between module eigengenes and different treatment of mice model were calculated to identify modules of interest which were significantly associated with the treatment of mice model.

Cell-Cell communication analyses : To investigate cell-cell communication between MII oocyte and ovary cells, 'CellChat' R package was performed to analysis the ligand and receptor between oocyte and ovary. Ligand-receptor pairs are defined based on 'CellChatDB' database. Based on biological function, all the interactions are grouped into 229 signaling pathway families. The defferentially expressed signaling genes were identified by Wilcoxon rank sum test with significance level of 0.05.

Metabolic pathway analysis of MII oocyte: MII oocytes metabolic pathway quantification was conducted by 'scMetabolism' R package**.** The function AUCell was used to quantify the metabolic activity after implement with Seurat pipeline. The genes for pathway analyses can be found online (https://github.com/wu-yc/scMetabolism).

Funding:
Swedish Medical Research Council: project no. 2018-02435 (ESV), 2018-02557 and 2020-00253 (QD)
Knut and Alice Wallenberg Foundation: 2019.0211 (QD)
Karolinska Instiutet faculty funded position (QD)
Novo Nordisk Foundation: NNF19OC0056647 and and NNF22OC0072904 (ESV)
Strategic Research Program in Diabetes at the Karolinska Institutet (ESV)
Diabetes Foundation: DIA2021-633 (ESV)
Karolinska Institutet KID funding: 2020-00990 (ESV)
Regional Agreement on Medical Training and Clinical Research between the Stockholm County Council and the Karolinska Institutet: 20190079 (ESV)

Author contributions:
Y.P performed sequencing library preparation and computational analyses, interpretated data, prepared figures and assist in writing the manuscript; S.R. designed the study, collected mouse tissues and MII oocytes, analyzed data, prepared figures, and wrote the manuscript; H.J. analyzed the human and mice RNAseq data in adipose tissue and prepared figures; HL and EL collected mouse tissues; Q.D. and E.S-V. designed and supervised the study, interpreted data and wrote the manuscript.

Competing interests: Authors declare that they have no competing interests.

References

Altinkaya, S.O. (2021). Galanin and glypican-4 levels depending on metabolic and cardiovascular risk factors in patients with polycystic ovary syndrome. Archives of endocrinology and metabolism *65*, 479-487.

Au - Xue, P., Au - Wang, Z., Au - Fu, X., Au - Wang, J., Au - Punchhi, G., Au - Wolfe, A., and Au - Wu, S. (2018). A Hyperandrogenic Mouse Model to Study Polycystic Ovary Syndrome. JoVE, e58379.

Barrett, E.S., Hoeger, K.M., Sathyanarayana, S., Abbott, D.H., Redmon, J.B., Nguyen, R.H.N., and Swan, S.H. (2018). Anogenital distance in newborn daughters of women with polycystic ovary syndrome indicates fetal testosterone exposure. J Dev Orig Health Dis *9*, 307-314.

Caldwell, A.S.L., Middleton, L.J., Jimenez, M., Desai, R., McMahon, A.C., Allan, C.M., Handelsman, D.J., and Walters, K.A. (2014). Characterization of Reproductive, Metabolic, and Endocrine Features of Polycystic Ovary Syndrome in Female Hyperandrogenic Mouse Models. Endocrinology *155*, 3146-3159.

Chen, C.C., Lee, T.Y., Kwok, C.F., Hsu, Y.P., Shih, K.C., Lin, Y.J., and Ho, L.T. (2015). Major urinary protein 1 interacts with cannabinoid receptor type 1 in fatty acid-induced hepatic insulin resistance in a mouse hepatocyte model. Biochemical and biophysical research communications *460*, 1063-1068.

Chen, J., Spracklen, C.N., Marenne, G., Varshney, A., Corbin, L.J., Luan, J., Willems, S.M., Wu, Y., Zhang, X., Horikoshi, M.*, et al.* (2021). The trans-ancestral genomic architecture of glycemic traits. Nat Genet *53*, 840-860.

Coyle, C.S., Prescott, M., Handelsman, D.J., Walters, K.A., and Campbell, R.E. (2022). Chronic androgen excess in female mice does not impact luteinizing hormone pulse frequency or putative GABAergic inputs to GnRH neurons. Journal of Neuroendocrinology *34*, e13110.

Dadachanji, R., Shaikh, N., Khavale, S., Patil, A., Shah, N., and Mukherjee, S. (2015). PON1 polymorphisms are associated with polycystic ovary syndrome susceptibility, related traits, and PON1 activity in Indian women with the syndrome. Fertility and sterility *104*, 207-216.

Dapas, M., and Dunaif, A. (2020). The contribution of rare genetic variants to the pathogenesis of polycystic ovary syndrome. Current opinion in endocrine and metabolic research *12*, 26-32.

Dapas, M., and Dunaif, A. (2022a). Deconstructing a Syndrome: Genomic Insights into PCOS Causal Mechanisms and Classification. Endocr Rev.

Dapas, M., and Dunaif, A. (2022b). Deconstructing a Syndrome: Genomic Insights Into PCOS Causal Mechanisms and Classification. Endocrine Reviews.

Dapas, M., Lin, F.T.J., Nadkarni, G.N., Sisk, R., Legro, R.S., Urbanek, M., Hayes, M.G., and Dunaif, A. (2020). Distinct subtypes of polycystic ovary syndrome with novel genetic associations: An unsupervised, phenotypic clustering analysis. PLoS medicine *17*, e1003132.

Day, F., Karaderi, T., Jones, M.R., Meun, C., He, C., Drong, A., Kraft, P., Lin, N., Huang, H., Broer, L.*, et al.* (2018). Large-scale genome-wide meta-analysis of polycystic ovary syndrome suggests shared genetic architecture for different diagnosis criteria. PLOS Genetics *14*, e1007813.

Dissen, G.A., Garcia-Rudaz, C., Paredes, A., Mayer, C., Mayerhofer, A., and Ojeda, S.R. (2009). Excessive ovarian production of nerve growth factor facilitates development of cystic ovarian morphology in mice and is a feature of polycystic ovarian syndrome in humans. Endocrinology *150*, 2906-2914.

Divoux, A., Erdos, E., Whytock, K., Osborne, T.F., and Smith, S.R. (2022). Transcriptional and DNA Methylation Signatures of Subcutaneous Adipose Tissue and Adipose-Derived Stem Cells in PCOS Women. Cells *11*.
Dunaif, A. (2016). Perspectives in Polycystic Ovary Syndrome: From Hair to Eternity. The Journal of Clinical Endocrinology & Metabolism *101*, 759-768.
Escobar-Morreale, H.F. (2018). Polycystic ovary syndrome: definition, aetiology, diagnosis and treatment. Nature Reviews Endocrinology *14*, 270-284.
Flannick, J., and Florez, J.C. (2016). Type 2 diabetes: genetic data sharing to advance complex disease research. Nat Rev Genet *17*, 535-549.
Fornes, R., Manti, M., Qi, X., Vorontsov, E., Sihlbom, C., Nystrom, J., Jerlhag, E., Maliqueo, M., Hirschberg, A.L., Carlstrom, M*., et al.* (2019). Mice exposed to maternal androgen excess and diet-induced obesity have altered phosphorylation of catechol-O-methyltransferase in the placenta and fetal liver. International journal of obesity.
Franks, S., and Hardy, K. (2018). Androgen Action in the Ovary. Front Endocrinol (Lausanne) *9*, 452.
Gilchrist, R.B., Lane, M., and Thompson, J.G. (2008). Oocyte-secreted factors: regulators of cumulus cell function and oocyte quality. Human reproduction update *14*, 159-177.
Han, L., Ren, C., Li, L., Li, X., Ge, J., Wang, H., Miao, Y.L., Guo, X., Moley, K.H., Shu, W*., et al.* (2018). Embryonic defects induced by maternal obesity in mice derive from Stella insufficiency in oocytes. Nat Genet *50*, 432-442.
Harwood, J.C., Leonenko, G., Sims, R., Escott-Price, V., Williams, J., and Holmans, P. (2021). Defining functional variants associated with Alzheimer's disease in the induced immune response. Brain communications *3*, fcab083.
Homburg, R., Gudi, A., Shah, A., and A, M.L. (2017). A novel method to demonstrate that pregnant women with polycystic ovary syndrome hyper-expose their fetus to androgens as a possible stepping stone for the developmental theory of PCOS. A pilot study. Reproductive biology and endocrinology : RB&E *15*, 61.
Jin, S., Guerrero-Juarez, C.F., Zhang, L., Chang, I., Ramos, R., Kuan, C.-H., Myung, P., Plikus, M.V., and Nie, Q. (2021). Inference and analysis of cell-cell communication using CellChat. Nature Communications *12*, 1088.
Kakoly, N.S., Khomami, M.B., Joham, A.E., Cooray, S.D., Misso, M.L., Norman, R.J., Harrison, C.L., Ranasinha, S., Teede, H.J., and Moran, L.J. (2018). Ethnicity, obesity and the prevalence of impaired glucose tolerance and type 2 diabetes in PCOS: a systematic review and meta-regression. Human reproduction update *24*, 455-467.
Kang, H.S., Liao, G., DeGraff, L.M., Gerrish, K., Bortner, C.D., Garantziotis, S., and Jetten, A.M. (2013). CD44 plays a critical role in regulating diet-induced adipose inflammation, hepatic steatosis, and insulin resistance. PloS one *8*, e58417.
Khristi, V., Chakravarthi, V.P., Singh, P., Ghosh, S., Pramanik, A., Ratri, A., Borosha, S., Roby, K.F., Wolfe, M.W., and Rumi, M.A.K. (2018). ESR2 regulates granulosa cell genes essential for follicle maturation and ovulation. Molecular and cellular endocrinology *474*, 214-226.
Knoedler, J.R., Inoue, S., Bayless, D.W., Yang, T., Tantry, A., Davis, C.-h., Leung, N.Y., Parthasarathy, S., Wang, G., Alvarado, M*., et al.* (2022). A functional cellular framework for sex and estrous cycle-dependent gene expression and behavior. Cell *185*, 654-671.e622.
Li, L., Zhu, S., Shu, W., Guo, Y., Guan, Y., Zeng, J., Wang, H., Han, L., Zhang, J., Liu, X*., et al.* (2020). Characterization of Metabolic Patterns in Mouse Oocytes during Meiotic Maturation. Molecular cell *80*, 525-540.e529.
Liu, Q., Zhu, Z., Kraft, P., Deng, Q., Stener-Victorin, E., and Jiang, X. (2022). Genomic correlation, shared loci, and causal relationship between obesity and polycystic ovary syndrome: a large-scale genome-wide cross-trait analysis. BMC medicine *20*, 66.

Magro-Lopez, E., and Muñoz-Fernández, M. (2021). The Role of BMP Signaling in Female Reproductive System Development and Function. International journal of molecular sciences *22*.
Manti, M., Fornes, R., Pironti, G., McCann Haworth, S., Zhengbing, Z., Benrick, A., Carlstrom, M., Andersson, D., and Stener-Victorin, E. (2019a). Maternal androgen excess induces cardiac hypertrophy and left ventricular dysfunction in female mice offspring. Cardiovascular research.
Manti, M., Fornes, R., Pironti, G., McCann Haworth, S., Zhengbing, Z., Benrick, A., Carlström, M., Andersson, D., and Stener-Victorin, E. (2019b). Maternal androgen excess induces cardiac hypertrophy and left ventricular dysfunction in female mice offspring. Cardiovascular research *116*, 619-632.
Manti, M., Fornes, R., Qi, X., Folmerz, E., Linden Hirschberg, A., de Castro Barbosa, T., Maliqueo, M., Benrick, A., and Stener-Victorin, E. (2018a). Maternal androgen excess and obesity induce sexually dimorphic anxiety-like behavior in the offspring. FASEB journal : official publication of the Federation of American Societies for Experimental Biology *32*, 4158-4171.
Manti, M., Fornes, R., Qi, X., Folmerz, E., Linden Hirschberg, A., de Castro Barbosa, T., Maliqueo, M., Benrick, A., and Stener-Victorin, E. (2018b). Maternal androgen excess and obesity induce sexually dimorphic anxiety-like behavior in the offspring. Faseb J, fj201701263RR.
Manti, M., Pui, H.P., Edström, S., Risal, S., Lu, H., Lindgren, E., Ohlsson, C., Jerlhag, E., Benrick, A., Deng, Q.*, et al.* (2020). Excess of ovarian nerve growth factor impairs embryonic development and causes reproductive and metabolic dysfunction in adult female mice. FASEB journal : official publication of the Federation of American Societies for Experimental Biology *34*, 14440-14457.
March, W.A., Moore, V.M., Willson, K.J., Phillips, D.I., Norman, R.J., and Davies, M.J. (2010). The prevalence of polycystic ovary syndrome in a community sample assessed under contrasting diagnostic criteria. Hum Reprod *25*, 544-551.
McCartney, C.R., and Marshall, J.C. (2016). Polycystic Ovary Syndrome. New England Journal of Medicine *375*, 54-64.
Moore, A.M., Prescott, M., Marshall, C.J., Yip, S.H., and Campbell, R.E. (2015). Enhancement of a robust arcuate GABAergic input to gonadotropin-releasing hormone neurons in a model of polycystic ovarian syndrome. Proceedings of the National Academy of Sciences *112*, 596-601.
Nisenblat, V., and Norman, R.J. (2009). Androgens and polycystic ovary syndrome. Current opinion in endocrinology, diabetes, and obesity *16*, 224-231.
Palomba, S., Marotta, R., Di Cello, A., Russo, T., Falbo, A., Orio, F., Tolino, A., Zullo, F., Esposito, R., and La Sala, G.B. (2012). Pervasive developmental disorders in children of hyperandrogenic women with polycystic ovary syndrome: a longitudinal case-control study. Clinical endocrinology *77*, 898-904.
Perovic Blagojevic, I.M., Vekic, J.Z., Macut, D.P., Ignjatovic, S.D., Miljkovic-Trailovic, M.M., Zeljkovic, A.R., Spasojevic-Kalimanovska, V.V., Bozic-Antic, I.B., Bjekic-Macut, J.D., Kastratovic-Kotlica, B.A.*, et al.* (2021). Overweight and obesity in polycystic ovary syndrome: association with inflammation, oxidative stress and dyslipidaemia. British Journal of Nutrition, 1-9.
Priest, C., and Tontonoz, P. (2019). Inter-organ cross-talk in metabolic syndrome. Nature Metabolism *1*, 1177-1188.
Risal, S., Manti, M., Lu, H., Fornes, R., Larsson, H., Benrick, A., Deng, Q., Cesta, C.E., Rosenqvist, M.A., and Stener-Victorin, E. (2021). Prenatal androgen exposure causes a

sexually dimorphic transgenerational increase in offspring susceptibility to anxiety disorders. Transl Psychiatry *11*, 45.
Risal, S., Pei, Y., Lu, H., Manti, M., Fornes, R., Pui, H.-P., Zhao, Z., Massart, J., Ohlsson, C., Lindgren, E.*, et al.* (2019). Prenatal androgen exposure and transgenerational susceptibility to polycystic ovary syndrome. Nature Medicine *25*, 1894-1904.
Ruth, K.S., Day, F.R., Tyrrell, J., Thompson, D.J., Wood, A.R., Mahajan, A., Beaumont, R.N., Wittemans, L., Martin, S., Busch, A.S.*, et al.* (2020). Using human genetics to understand the disease impacts of testosterone in men and women. Nature Medicine *26*, 252-258.
Saben, J.L., Boudoures, A.L., Asghar, Z., Thompson, A., Drury, A., Zhang, W., Chi, M., Cusumano, A., Scheaffer, S., and Moley, K.H. (2016). Maternal Metabolic Syndrome Programs Mitochondrial Dysfunction via Germline Changes across Three Generations. Cell reports *16*, 1-8.
Sano, T., Sanada, T., Sotomaru, Y., Shinjo, T., Iwashita, M., Yamashita, A., Fukuda, T., Sanui, T., Asano, T., Kanematsu, T.*, et al.* (2019). Ccr7 null mice are protected against diet-induced obesity via Ucp1 upregulation and enhanced energy expenditure. Nutrition & Metabolism *16*, 43.
Shi, Y., Zhao, H., Shi, Y., Cao, Y., Yang, D., Li, Z., Zhang, B., Liang, X., Li, T., Chen, J.*, et al.* (2012). Genome-wide association study identifies eight new risk loci for polycystic ovary syndrome. Nat Genet *44*, 1020-1025.
Shimogori, T., Lee, D.A., Miranda-Angulo, A., Yang, Y., Wang, H., Jiang, L., Yoshida, A.C., Kataoka, A., Mashiko, H., Avetisyan, M.*, et al.* (2010). A genomic atlas of mouse hypothalamic development. Nature Neuroscience *13*, 767-775.
Stener-Victorin, E., and Deng, Q. (2021). Epigenetic inheritance of polycystic ovary syndrome - challenges and opportunities for treatment. Nat Rev Endocrinol *17*, 521-533.
Stener-Victorin, E., Padmanabhan, V., Walters, K.A., Campbell, R.E., Benrick, A., Giacobini, P., Dumesic, D.A., and Abbott, D.H. (2020). Animal Models to Understand the Etiology and Pathophysiology of Polycystic Ovary Syndrome. Endocrine Reviews *41*, 538-576.
Sullivan, S.D., and Moenter, S.M. (2004). Prenatal androgens alter GABAergic drive to gonadotropin-releasing hormone neurons: Implications for a common fertility disorder. Proceedings of the National Academy of Sciences of the United States of America *101*, 7129-7134.
Teede, H.J., Misso, M.L., Costello, M.F., Dokras, A., Laven, J., Moran, L., Piltonen, T., and Norman, R.J. (2018). Recommendations from the international evidence-based guideline for the assessment and management of polycystic ovary syndrome. Hum Reprod *33*, 1602-1618.
van Houten, E.L., Kramer, P., McLuskey, A., Karels, B., Themmen, A.P., and Visser, J.A. (2012). Reproductive and metabolic phenotype of a mouse model of PCOS. Endocrinology *153*, 2861-2869.
Walters, K.A., Allan, C.M., and Handelsman, D.J. (2012). Rodent Models for Human Polycystic Ovary Syndrome1. Biology of Reproduction *86*.
Wang, J., Tang, J., Wang, B., Song, J., Liu, J., Wei, Z., Zhang, F., Ma, X., and Cao, Y. (2009). FABP4: a novel candidate gene for polycystic ovary syndrome. Endocrine *36*, 392-396.
Wang, Z., Shen, M., Xue, P., DiVall, S.A., Segars, J., and Wu, S. (2018). Female Offspring From Chronic Hyperandrogenemic Dams Exhibit Delayed Puberty and Impaired Ovarian Reserve. Endocrinology *159*, 1242-1252.
Warzych, E., and Lipinska, P. (2020). Energy metabolism of follicular environment during oocyte growth and maturation. The Journal of reproduction and development *66*, 1-7.
Wilson, J.L., Chen, W., Dissen, G.A., Ojeda, S.R., Cowley, M.A., Garcia-Rudaz, C., and Enriori, P.J. (2014). Excess of Nerve Growth Factor in the Ovary Causes a Polycystic Ovary-

941 Like Syndrome in Mice, which Closely Resembles Both Reproductive and Metabolic Aspects
942 of the Human Syndrome. Endocrinology *155*, 4494-4506.
943 Wurmbach, E., Yuen, T., Ebersole, B.J., and Sealfon, S.C. (2001). Gonadotropin-releasing
944 Hormone Receptor-coupled Gene Network Organization*210. Journal of Biological
945 Chemistry *276*, 47195-47201.
946
947 Hagemann-Jensen, M., Ziegenhain, C., Chen, P., Ramsköld, D., Hendriks, G.-J., Larsson,
948 A.J.M., Faridani, O.R., and Sandberg, R. (2020). Single-cell RNA counting at allele and
949 isoform resolution using Smart-seq3. Nat. Biotechnol. *38*, 708–714.

950 Langfelder, P., and Horvath, S. (2008). WGCNA: an R package for weighted correlation
951 network analysis. BMC Bioinformatics *9*, 559.

952 Parekh, S., Ziegenhain, C., Vieth, B., Enard, W., and Hellmann, I. (2018). zUMIs - A fast and
953 flexible pipeline to process RNA sequencing data with UMIs. GigaScience *7*.

954

Figure1 a

Summary of phenotypes of different PCOS-like mouse model (based published on literatures)								
Model	Reproductive phenotypes			Endocrine phenotype	Metabolic phenotype			Ref
	Disrupted estrous cycle	Oligo or anovulation	Polycystic ovaries	Hyperandrogenism	Fat mass	Adipocyte size	Glucose intolerance/Insulin resistance	
PNA (250 mg DHT -->E16.5-E18.5)	√	√	√/×	√/×	√	√	×	Risal et al., 2019; Moore et al., 2015; Sullivan and Moenter, 2004
Prepubertal androgenized (sc DHT pellet)	√	√	√	√/×	√	√	√	Caldwell et al., 2014
Nerve growth factor overexpression in theca cells (17NF)	√	N/A	√	√	√	√	√	Dissen et al., 2009; Manti et al., 2018a; Manti et al., 2020; Wilson et al., 2014
Maternal obesity (F_0-->F_1 female offspring)	√	N/A	×	×	√	√	×	Risal et al., 2019

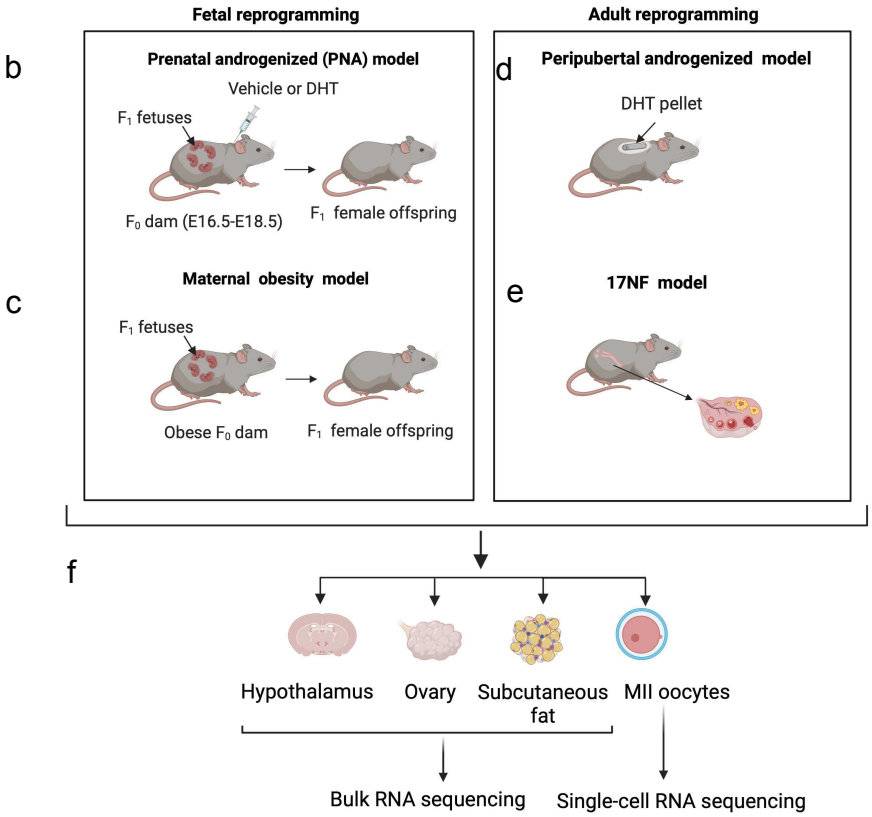

Fig. 1. Summary of metabolic and reproductive phenotype and Illustration of three PCOS mouse models and a maternal high fat high sugar (HFHS)-treated mouse model for comparative transcriptomic analyses of collected target tissues and MII oocytes. (a) Summary of metabolic and reproductive phenotype of Prenatal androgenized (PNA), Peripubertal androgenized, 17NF, and Maternal obesity **(b)** PNA in which F1 female offspring was analyzed. **(c)** F1 female offspring of HFHS diet induced maternal obese model.**(d)** Peripubertal androgenized (subcutaneous DHT implant), and **(e)** 17NF-model: theca-cell specific nerve growth factor (NGF) overexpressing transgenic mouse models. **(f)** Different targeted tissues, namely hypothalamus, ovaries, and subcutaneous adipose tissue used for transcriptomic analysis by bulk mRNA sequencing. Metaphase II (MII) oocytes are used for single-cell mRNA sequencing.

Figure 2

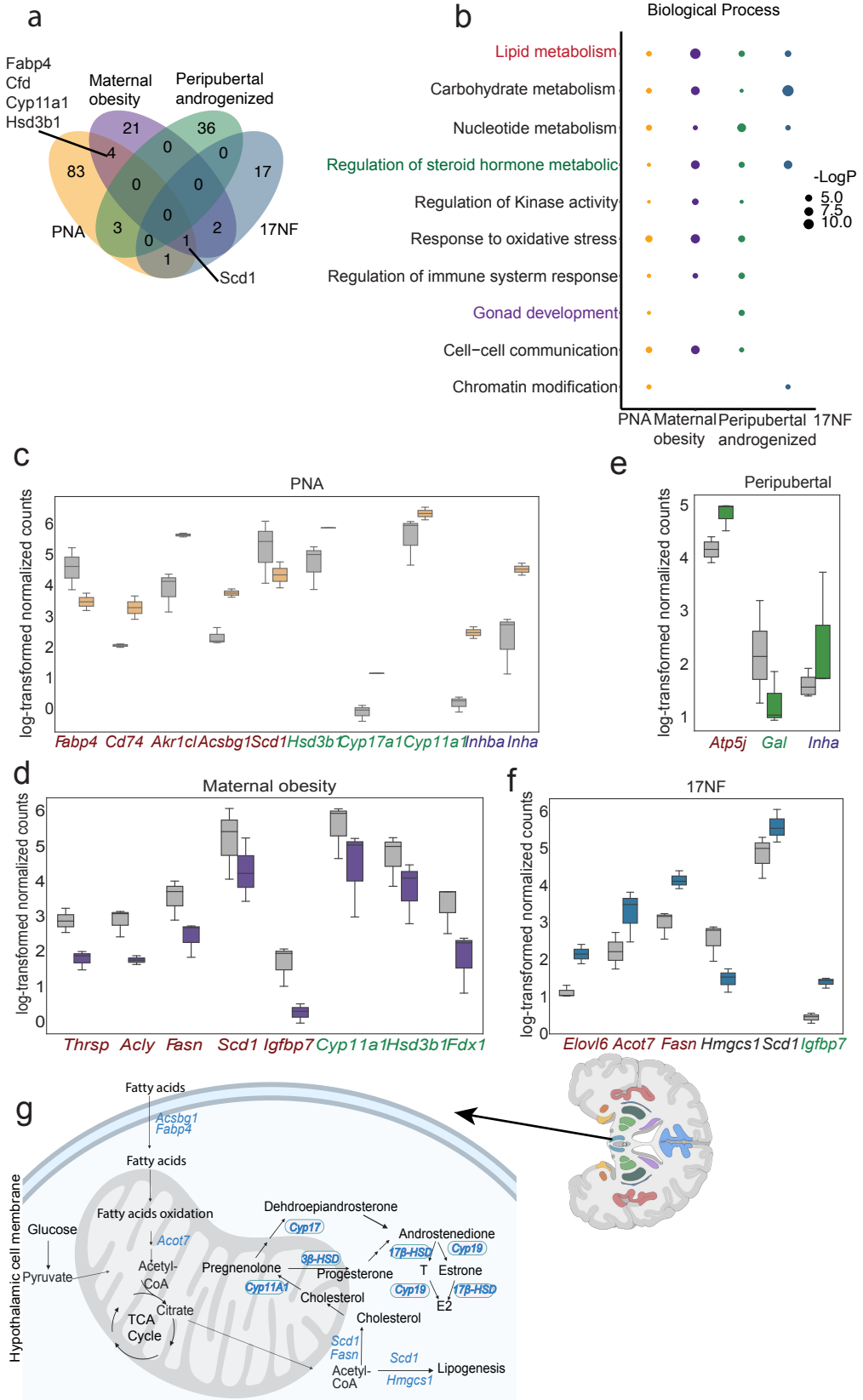
a
Fabp4
Cfd
Cyp11a1
Hsd3b1
Maternal obesity
Peripubertal androgenized
PNA
17NF
Scd1
b
Biological Process
Lipid metabolism
Carbohydrate metabolism
Nucleotide metabolism
Regulation of steroid hormone metabolic
Regulation of Kinase activity
Response to oxidative stress
Regulation of immune systerm response
Gonad development
Cell−cell communication
Chromatin modification
-LogP
5.0
7.5
10.0
PNA
Maternal obesity
Peripubertal androgenized
17NF
c
PNA
log-transformed normalized counts
Fabp4 Cd74 Akr1c1 Acsbg1 Scd1 Hsd3b1 Cyp17a1 Cyp11a1 Inhba Inha
d
Maternal obesity
log-transformed normalized counts
Thrsp Acly Fasn Scd1 Igfbp7 Cyp11a1 Hsd3b1 Fdx1
e
Peripubertal
log-transformed normalized counts
Atp5j Gal Inha
f
17NF
log-transformed normalized counts
Elovl6 Acot7 Fasn Hmgcs1 Scd1 Igfbp7
g
Hypothalamic cell membrane
Fatty acids
Acsbg1
Fabp4
Fatty acids
Fatty acids oxidation
Acot7
Glucose
Pyruvate
Acetyl-CoA
Citrate
TCA Cycle
Dehydroepiandrosterone
Cyp17
Androstenedione
17β-HSD
Cyp19
3β-HSD
Pregnenolone
Progesterone
T
Estrone
Cyp11A1
Cholesterol
Cyp19
17β-HSD
E2
Cholesterol
Scd1
Fasn
Acetyl-CoA
Scd1
Hmgcs1
Lipogenesis

Fig. 2. Common and distinct transcriptomic signature of hypothalamus. (a) Venn diagram of DEGs across all animal models (PNA model, n= 3 in control + vehicle, n= 2 in prenatal DHT; maternal obesity, n = 3 in control, n = 3 in maternal obesity; Peripubertal androgenized model, n = 3 in control + vehicle, n = 3 in Peripubertal DHT; 17NF, n=3 in control, n = 3 in 17NF). **(b)** Comparison of enriched gene ontology terms of DEGs across all animal models. **(c-f)** Bar plot showing expression level of DEGs enriched in lipid metabolism, steroid hormone metabolism and gonad development in PNA, Peripubertal androgenized, 17NF and maternal obesity, respectively. (g) Illustration of DEGs involved in lipid and steroid metabolism pathways in hypothalamus.

Figure 3

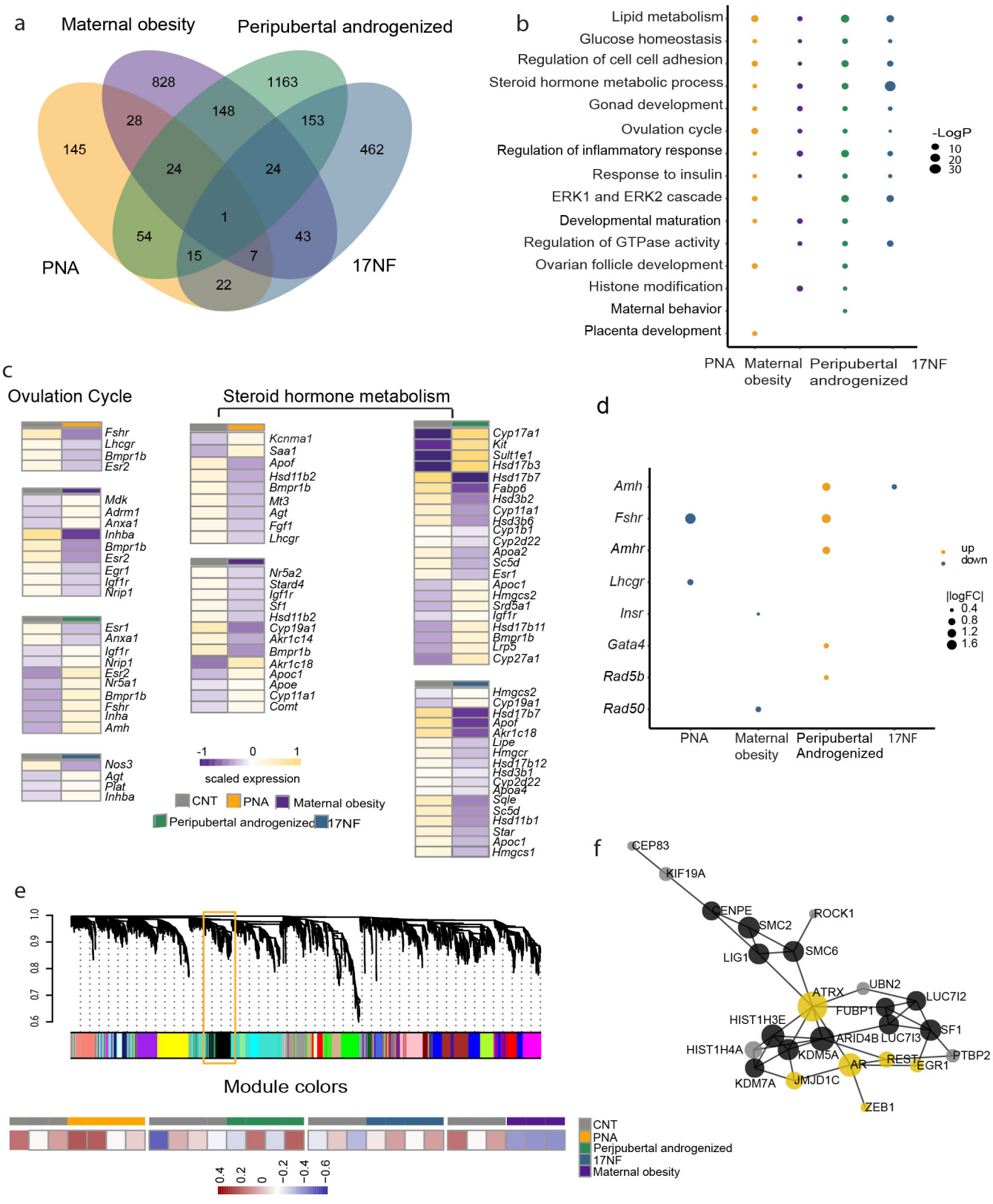
a
Maternal obesity
Peripubertal androgenized
PNA
17NF
828
1163
28
148
153
145
462
24
24
1
54
43
15
7
22
b
Lipid metabolism
Glucose homeostasis
Regulation of cell cell adhesion
Steroid hormone metabolic process
Gonad development
Ovulation cycle
Regulation of inflammatory response
Response to insulin
ERK1 and ERK2 cascade
Developmental maturation
Regulation of GTPase activity
Ovarian follicle development
Histone modification
Maternal behavior
Placenta development
-LogP
10
20
30
PNA
Maternal obesity
Peripubertal androgenized
17NF
c
Ovulation Cycle
Steroid hormone metabolism
Fshr
Lhcgr
Bmpr1b
Esr2
Mdk
Adrm1
Anxa1
Inhba
Bmpr1b
Esr2
Egr1
Igf1r
Nrip1
Esr1
Anxa1
Igf1r
Nrip1
Esr2
Nr5a1
Bmpr1b
Fshr
Inha
Amh
Nos3
Agt
Plat
Inhba
Kcnma1
Saa1
Apof
Hsd11b2
Bmpr1b
Mt3
Agt
Fgf1
Lhcgr
Nr5a2
Stard4
Igf1r
Sf1
Hsd11b2
Cyp19a1
Akr1c14
Bmpr1b
Akr1c18
Apoc1
Apoe
Cyp11a1
Comt
Cyp17a1
Kit
Sult1e1
Hsd17b3
Hsd17b7
Fabp6
Hsd3b2
Cyp11a1
Hsd3b6
Cyp1b1
Cyp2d22
Apoa2
Sc5d
Esr1
Apoc1
Hmgcs2
Srd5a1
Igf1r
Hsd17b11
Bmpr1b
Lrp5
Cyp27a1
Hmgcs2
Cyp19a1
Hsd17b7
Apof
Akr1c18
Lipe
Hmgcr
Hsd17b12
Hsd3b1
Cyp2d22
Apoa4
Sqle
Sc5d
Hsd11b1
Star
Apoc1
Hmgcs1
-1
0
1
scaled expression
CNT
PNA
Maternal obesity
Peripubertal androgenized
17NF
d
Amh
Fshr
Amhr
Lhcgr
Insr
Gata4
Rad5b
Rad50
up
down
|logFC|
0.4
0.8
1.2
1.6
PNA
Maternal obesity
Peripubertal Androgenized
17NF
e
1.0
0.9
0.8
0.7
0.6
Module colors
0.4
0.2
0
−0.2
−0.4
−0.6
CNT
PNA
Perjpubertal androgenized
17NF
Maternal obesity
f
CEP83
KIF19A
CENPE
SMC2
ROCK1
LIG1
SMC6
ATRX
UBN2
LUC7I2
FUBP1
HIST1H3E
SF1
ARID4B
LUC7I3
HIST1H4A
KDM5A
PTBP2
AR
REST
EGR1
KDM7A
JMJD1C
ZEB1

Fig. 3. Common and distinct transcriptomic signature of ovary. (a) Venn diagram of DEGs across all animal models (PNA model, n= 3 in control + vehicle, n= 4 in Prenatal DHT; Peripubertal androgenized model, n =4 in control + vehicle, n = 4 in Peripubertal DHT; 17NF, n=3 in control, n = 4 in 17NF; maternal obesity, n = 3 in control, n = 3 in maternal obesity). **(b)** Comparison of enriched gene ontology term of DEGs across all animal models. **(c)** Heatmap of expression of DEGs enriched in Ovulation cycle and Steroid hormone metabolism in PNA, maternal obesity, Peripubertal androgenized, and 17NF respectively. **(d)** Overlapped DEG genes of ovary tissue with GWAS genes women with PCOS in PNA, maternal obesity, Peripubertal androgenized, and17NF. **(e)** Module clustering tree diagram across animal models. Key module gene network involved in PCOS-like animal models. **(f)** Protein-Protein Interaction network of genes in black module (black module in e.). PPI Data are retrieved from String database.

Figure 4

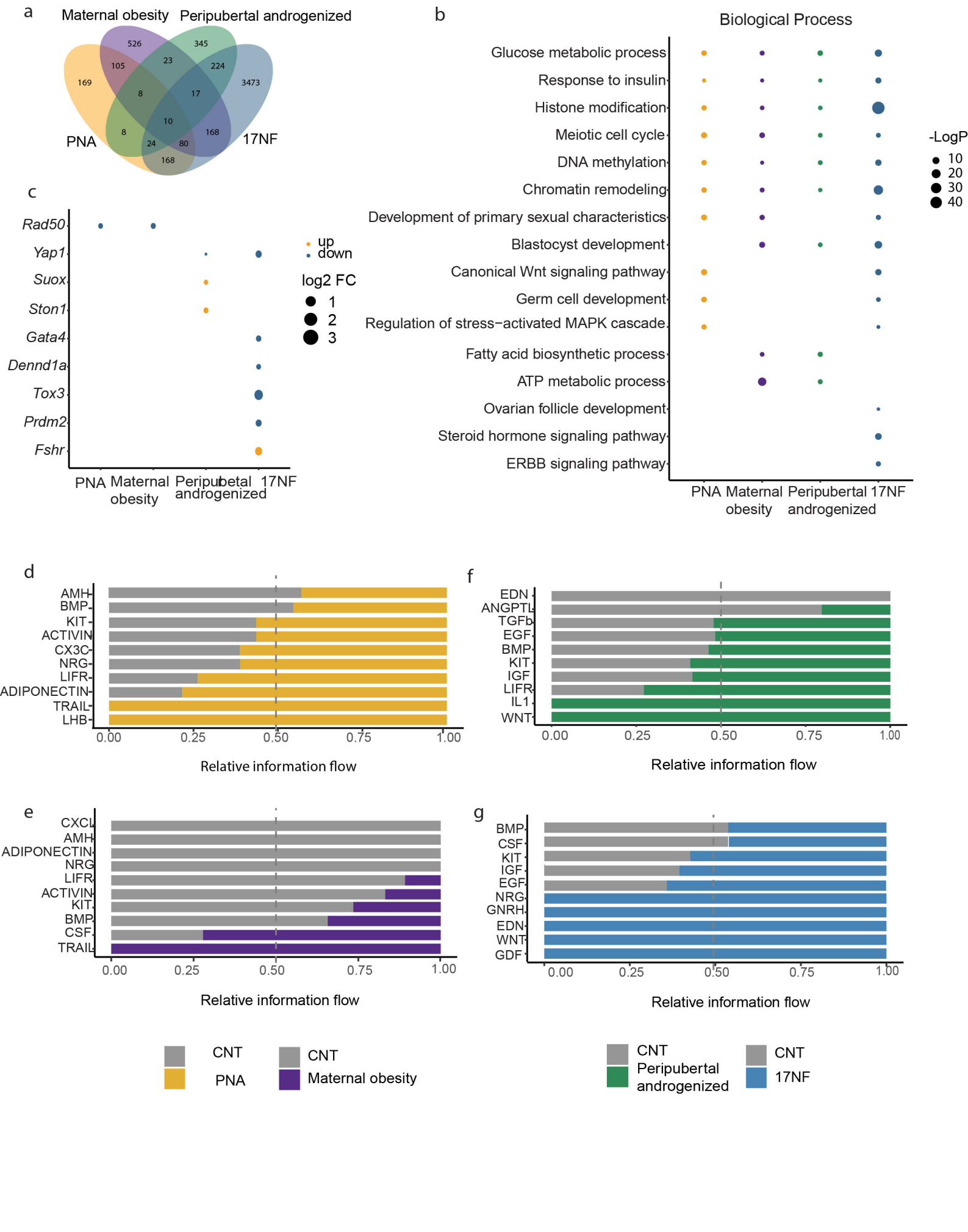
a
Maternal obesity
Peripubertal androgenized
PNA
17NF
526
345
105
23
224
169
3473
8
17
10
8
168
24
80
168
b
Biological Process
Glucose metabolic process
Response to insulin
Histone modification
Meiotic cell cycle
DNA methylation
Chromatin remodeling
Development of primary sexual characteristics
Blastocyst development
Canonical Wnt signaling pathway
Germ cell development
Regulation of stress−activated MAPK cascade
Fatty acid biosynthetic process
ATP metabolic process
Ovarian follicle development
Steroid hormone signaling pathway
ERBB signaling pathway
PNA
Maternal obesity
Peripubertal androgenized
17NF
-LogP
10
20
30
40
c
Rad50
Yap1
Suox
Ston1
Gata4
Dennd1a
Tox3
Prdm2
Fshr
up
down
log2 FC
1
2
3
PNA
Maternal obesity
Peripubertal androgenized
17NF
d
AMH
BMP
KIT
ACTIVIN
CX3C
NRG
LIFR
ADIPONECTIN
TRAIL
LHB
0.00
0.25
0.50
0.75
1.00
Relative information flow
f
EDN
ANGPTL
TGFb
EGF
BMP
KIT
IGF
LIFR
IL1
WNT
0.00
0.25
0.50
0.75
1.00
Relative information flow
e
CXCL
AMH
ADIPONECTIN
NRG
LIFR
ACTIVIN
KIT
BMP
CSF
TRAIL
0.00
0.25
0.50
0.75
1.00
Relative information flow
g
BMP
CSF
KIT
IGF
EGF
NRG
GNRH
EDN
WNT
GDF
0.00
0.25
0.50
0.75
1.00
Relative information flow
CNT
PNA
CNT
Maternal obesity
CNT
Peripubertal androgenized
CNT
17NF

Fig. 4. Common and distinct transcriptomic signature of MII oocytes. (a) Venn diagram of DEGs across all animal models (PNA model, n= 8 in control + vehicle, n= 10 in Prenatal DHT; maternal obesity, n = 8 in control, n = 15 in maternal obesity; Peripubertal androgenized model, n = 56 in control + vehicle, n = 67 in Peripubertal DHT; 17NF, n=16 in control, n = 16 in 17NF). **(b)** Comparison of enriched gene ontology term of DEGs in MII oocytes across all animal models. **(c)** Ovarlap DEG genes of MII oocytes with GWAS genes women with PCOS in PNA, Peripubertal androgenized, 17NF and maternal obesity. **(d-g)** Significant signalling pathways were ranked based on their differences of overall information flow within the inferred networks between control and treatment group in PNA, maternal obesity, Peripubertal androgenized and 17NF animal models, respectively.

Figure5

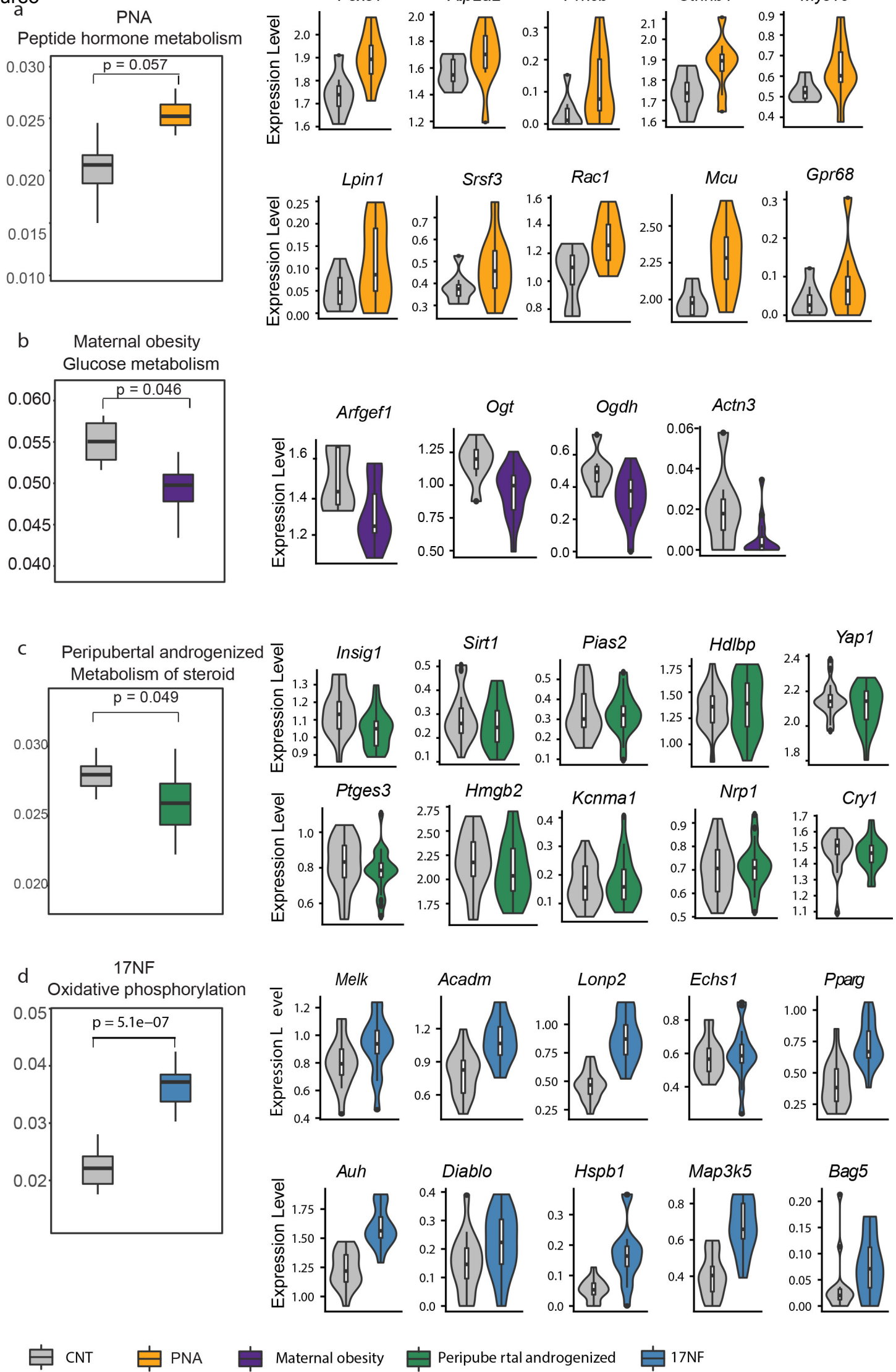
a
PNA
Peptide hormone metabolism
p = 0.057
Foxo1
Atp2a2
Prkcb
Ctnnb1
Myo1c
Lpin1
Srsf3
Rac1
Mcu
Gpr68
Expression Level
b
Maternal obesity
Glucose metabolism
p = 0.046
Arfgef1
Ogt
Ogdh
Actn3
c
Peripubertal androgenized
Metabolism of steroid
p = 0.049
Insig1
Sirt1
Pias2
Hdlbp
Yap1
Ptges3
Hmgb2
Kcnma1
Nrp1
Cry1
d
17NF
Oxidative phosphorylation
p = 5.1e−07
Melk
Acadm
Lonp2
Echs1
Pparg
Auh
Diablo
Hspb1
Map3k5
Bag5
CNT
PNA
Maternal obesity
Peripube rtal androgenized
17NF

Fig. 5. Metabolic pathway analysis of MII oocytes. (a-d) Significant metabolic pathways in PNA, Maternal obesity, Peripubertal androgenized and 17NF mice model respectively. Voilin plot shows the DEGs expression in each metabolic pathway.

Figure 6

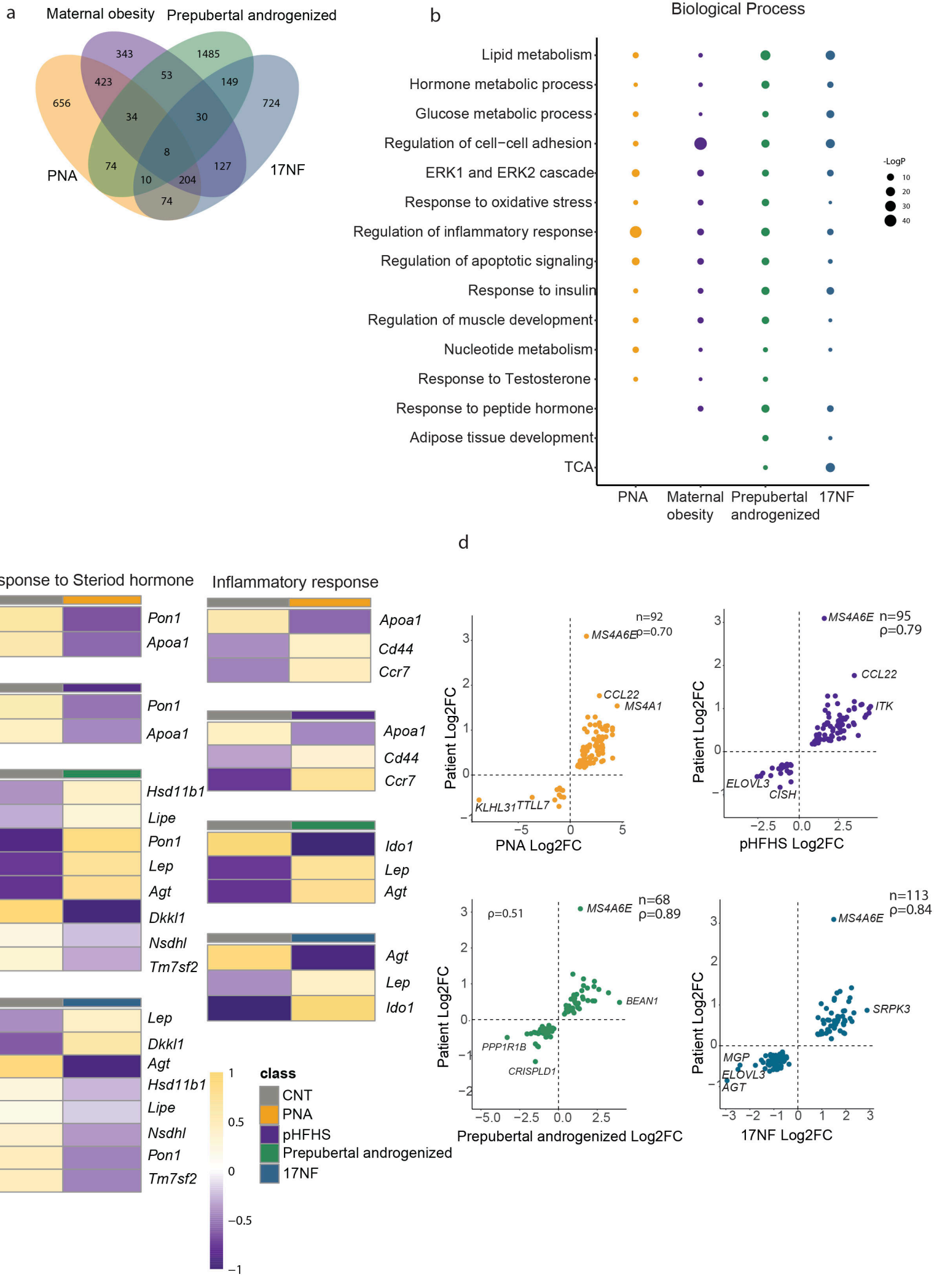
a
Maternal obesity
Prepubertal androgenized
PNA
17NF
343
1485
53
423
149
656
724
34
30
8
74
127
10
204
74
b
Biological Process
Lipid metabolism
Hormone metabolic process
Glucose metabolic process
Regulation of cell−cell adhesion
ERK1 and ERK2 cascade
Response to oxidative stress
Regulation of inflammatory response
Regulation of apoptotic signaling
Response to insulin
Regulation of muscle development
Nucleotide metabolism
Response to Testosterone
Response to peptide hormone
Adipose tissue development
TCA
PNA
Maternal obesity
Prepubertal androgenized
17NF
-LogP
10
20
30
40
c
Response to Steriod hormone
Inflammatory response
Pon1
Apoa1
Hsd11b1
Lipe
Lep
Agt
Dkkl1
Nsdhl
Tm7sf2
Cd44
Ccr7
Ido1
1
0.5
0
−0.5
−1
class
CNT
PNA
pHFHS
Prepubertal androgenized
17NF
d
n=92
ρ=0.70
MS4A6E
CCL22
MS4A1
KLHL31
TTLL7
Patient Log2FC
PNA Log2FC
n=95
ρ=0.79
ITK
ELOVL3
CISH
pHFHS Log2FC
ρ=0.51
n=68
ρ=0.89
BEAN1
PPP1R1B
CRISPLD1
Prepubertal androgenized Log2FC
n=113
ρ=0.84
SRPK3
MGP
AGT
17NF Log2FC

Fig. 6. Common and distinct transcriptomic signature of adipose tissue. (a) Venn diagram of DEGs across all animal models (PNA model, n= 3 in control + vehicle, n= 4 in Prenatal DHT; maternal obesity, n = 3 in control, n = 3 in maternal obesity; Peripubertal androgenized model, n =4 in control + vehicle, n = 4 in Peripubertal DHT; 17NF, n=3 in control, n = 3 in 17NF). **(b)** Comparison of enriched gene ontology term of DEGs in adipose tissue across all animal models. **(c)** Heatmap of expression of DEGs enriched in Response to steroid hormone, inflammatory response in PNA, maternal obesity, Peripubertal androgenized, and 17NF, respectively. **(d)** Scatter plot comparing alteration of gene expression between disease and controls in mouse models and patients (Divoux et al., 2022). Yellow dots indicate the genes whose expression alterations in mouse models are in line with patients. Blue dots indicate the genes whose expression alterations in mouse models are opposite to patients. The spearman correlation coefficient in corresponding group are also shown.

Figure 7

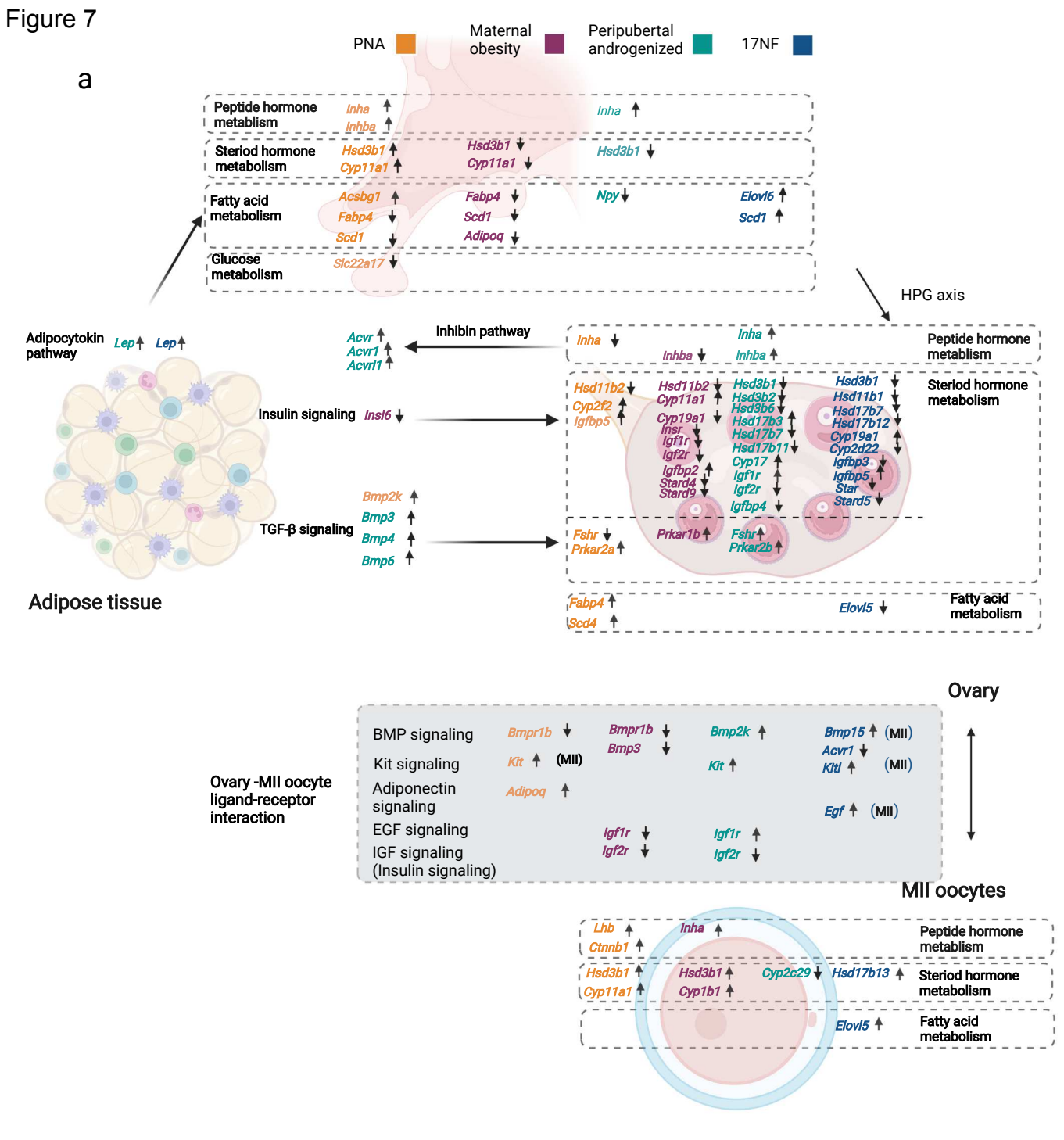
a
PNA
Maternal obesity
Peripubertal androgenized
17NF
Peptide hormone metablism
Inha
Inhba
Steriod hormone metabolism
Hsd3b1
Cyp11a1
Fatty acid metabolism
Acsbg1
Fabp4
Scd1
Adipoq
Npy
Elovl6
Glucose metabolism
Slc22a17
HPG axis
Adipocytokin pathway
Lep
Inhibin pathway
Acvr
Acvr1
Acvrl1
Insulin signaling
Insl6
TGF-β signaling
Bmp2k
Bmp3
Bmp4
Bmp6
Adipose tissue
Hsd11b2
Cyp2f2
Igfbp5
Cyp19a1
Insr
Igf1r
Igf2r
Igfbp2
Stard4
Stard9
Cyp17
Igf1r
Igf2r
Igfbp4
Hsd3b6
Hsd17b3
Hsd17b7
Hsd17b11
Hsd11b1
Hsd17b12
Cyp2d22
Igfbp3
Igfbp5
Star
Stard5
Fshr
Prkar2a
Prkar1b
Prkar2b
Elovl5
Ovary
Ovary -MII oocyte ligand-receptor interaction
BMP signaling
Kit signaling
Adiponectin signaling
EGF signaling
IGF signaling (Insulin signaling)
Bmpr1b
Bmp3
Kit
Adipoq
Igf1r
Igf2r
Bmp15
Acvr1
Kitl
Egf
(MII)
MII oocytes
Lhb
Ctnnb1
Cyp2c29
Hsd17b13
Cyp1b1

Fig. 7 Transcriptomic interaction among hypothalamus, ovary, adipose tissue and MII oocytes in PCOS-like models. (a) Transcriptomic cross-talk and unique gene signatures among hypothalamus, ovary, adipose tissue and MII oocytes in PNA, maternal obesity, Peripubertal androgenized and 17NF respectively.

Supplementary figure 1

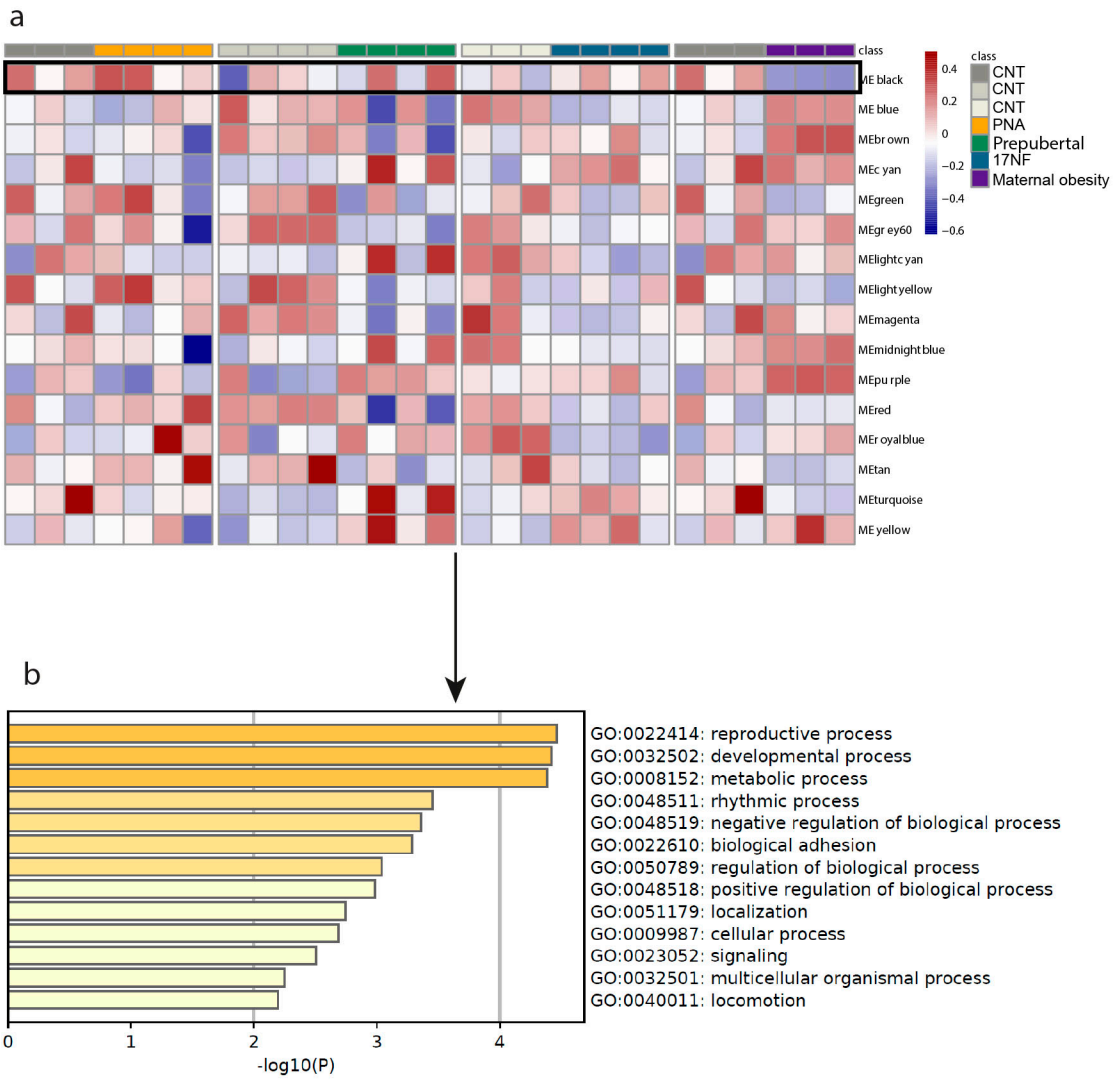

Supplementary Fig. S1. **(a)** Heatmap depicting the correlation between module eigengenes and PNA model, Peripubertal androgenized model, 17NF model and maternal obesity model phenotype. **(b)** GO enrichment analysis of selected module gene.

Supplementary figure 2

Supplementary Fig. S2. (a) Heatmap of expression of DEGs of adipose tissue enriched in glucose homeostasis in PNA, maternal obesity, Peripubertal androgenized, and 17NF, respectively.

Supplementary Files

This is a list of supplementary files associated with this preprint. Click to download.

- SupplementaryTableS1HypothalamusDEGgenes.xlsx
- SupplementaryTableS2GOHypothalaums.xlsx
- SupplementaryTableS3OvaryDEGs.xlsx
- SupplementaryTableS4OvaryGO.xlsx
- SupplementaryTableS5OvaryWGCNAtrainingmodulegenes.xlsx
- SupplementaryTableS6DEGsMIIoocytes.xlsx
- SupplementaryTableS7GOMIIoocytes.xlsx
- SupplementaryTableS8DEGsFat.xlsx
- SupplementaryTableS9GOtermAdipose.xlsx
- SupplementrayTableS10CommonDEGsinadiposetissuebetweenmousemodelsandwomenwithPCOS.xlsx
- SupplementaryTableS11DEGssharedacrosstissues.xlsx
- SupplementaryTableS12DEGsinsteroidhormonemetabolismregulation.xlsx
- SupplementaryTableS13comparisonofDEGsinfetalprogrammingversusadultprogramming.xlsx